

You Can't Always Check What You Wanted: Selective Checking and Trusted Execution to Prevent False Actuations in Cyber-Physical Systems

Monowar Hasan

School of Electrical Engineering & Computer Science
Washington State University, Pullman, WA, USA
Email: monowar.hasan@wsu.edu

Sibin Mohan

Department of Computer Science
The George Washington University, Washington, DC, USA
Email: sbin.mohan@gwu.edu

Abstract

Cyber-physical systems (CPS) are vulnerable to attacks targeting outgoing actuation commands that modify their physical behaviors. The limited resources in such systems, coupled with their stringent timing constraints, often prevents the checking of every outgoing command. We present a “selective checking” mechanism that uses game-theoretic modeling to identify the right subset of commands to be checked in order to deter an adversary. This mechanism is coupled with a “delay-aware” trusted execution environment (TEE) to ensure that only verified actuation commands are ever sent to the physical system, thus maintaining their safety and integrity. The *selective checking and trusted execution (SCATE)* framework is implemented on an off-the-shelf ARM platform running standard embedded Linux. We demonstrate the effectiveness of SCATE using four realistic cyber-physical systems (a ground rover, a flight controller, a robotic arm and an automated syringe pump) and study design trade-offs.

Not only does SCATE provide a high level of security and high performance, it also suffers from significantly lower overheads (30.48%–47.32% less) in the process. In fact, SCATE can work with more systems without negatively affecting the safety of the system. Considering that most CPS do not have any such checking mechanisms, and SCATE is *guaranteed* to meet all the timing requirements (*i.e.*, ensure the safety/integrity of the system), our methods can significantly improve the security (and, hence, safety) of the system.

I. INTRODUCTION

A large number of critical systems that are in operation today (*e.g.*, autonomous cars, avionics, drones, power grids, industrial control systems, medical devices, automobiles, space vehicles, *etc.*) can be classified as “cyber-physical systems” (CPS)¹. Such systems often have limited resources (processor, memory, battery life, *etc.*) and must also meet stringent *timing* constraints. For instance, an industrial robot on a manufacturing line, must carry out its operation (*e.g.*, placing an object on a conveyor) in 50–100 ms [1]. Failure to do so, could disrupt the entire manufacturing operation and even put the safety of the plant and human operators at risk!

Modern CPS with such “real-time” requirements are increasingly becoming targets for cyber-attacks. Traditional safety and fault-tolerance mechanisms used in real-time CPS were designed to counter random or accidental faults and failures and cannot deal with intentional cyber attacks orchestrated by an intelligent and capable adversary. Further, (*i*) the drive towards the use of standardized protocols and off-the-shelf components (for interoperability, reduced infrastructure and maintenance costs) and (*ii*) the emergence of smart and connected systems (*e.g.*, real-time Internet-of-things [2], smart grids [3], smart manufacturing [4], smart transportation [5], *etc.*) are increasing the attack surfaces available to adversaries. The traditional approaches of air-gapping such systems [6], [7] or using proprietary protocols and hardware [8] have been found wanting in the face of recent high-profile attacks: *e.g.*, Stuxnet [9], attack demonstrations by researchers on medical devices [10] and automobiles [11], denial-of-service (DoS) attacks mounted from IoT devices [12], among others.

A common thread among all of the aforementioned attacks, especially ones that threaten the physical safety of the system, is the *falsification of actuation commands* — *i.e.*, commands that control the state of the physical system are either modified or replaced while in transit to the physical component. Note that CPS are comprised of a tight interplay between computation, control and communication. At its core, a cyber-physical “plant” consists of actuators and sensors that, respectively, monitor and control the physical properties of the system. Due to the tight coupling between actuators and physical plants, such systems are often vulnerable to unexpected situations (*e.g.*, malicious actions) that were not considered during the design/development phases [13]. Hence, sending false/spoofed commands to the actuators can disrupt the normal operation of the physical plant and jeopardize its safety. In the manufacturing robot example mentioned earlier, the attacker could modify the command that changes the angle of rotation of the robot arm, thus causing it to completely miss the conveyor and, potentially, crash the entire system.

¹The term cyber-physical systems refers to the tight conjoining of and coordination between computational and physical resources.

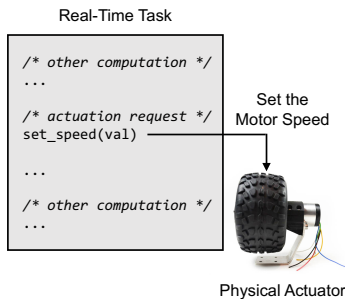


Fig. 1. Vanilla (non-secure) execution: does not check actuation commands.

We intend to *check actuation commands before they can affect the state of the physical system*. If we find that the command can have negative effects, *i.e.*, it compromises the safety and/or integrity of the CPS, then we prevent it from being sent out.² To prevent tampering, we *implement the checking mechanism in a trusted execution environment (TEE)* that is available on modern commodity processors, *viz.*, the ARM TrustZone [14]³. In an ideal scenario, every outgoing actuation command should be checked. A serious hurdle that prevents such a strategy is that, as mentioned earlier, CPS have stringent timing requirements — very often the actuation command, once sent out, *must be received by the physical system in a short, fixed, amount of time*. This limits the amount of time delays that can be introduced during the checking process. In addition, the control software has its own timing constraints, *e.g.*, it must complete execution before a certain “deadline”; failure to do so can also cause instability in the system. Hence, we *cannot check (and thus, delay) every command* since each check compounds the delays faced by the system. In addition, as seen in Sec. III-A, the use of the TEE-based checking mechanism introduces additional delays due to context-switch overheads, further (negatively) affecting the deadlines.

Hence, there is a need to carefully consider *how many* and *which* actuation commands are to be checked — to ensure that (a) the system safety/timing requirements are met and (b) also deter attackers. Picking a fixed subset of actuation commands is not helpful since an adversary can circumvent the checks by targeting the “unchecked” commands. To this end, *we develop a mechanism to validate a random subset of commands, varying at run-time* that significantly increases the difficulty for would-be attackers. We use a *game-theoretic formulation* of a two-player normal-form game [16]–[18] for the “selective checking” of the actuation commands (Sec. IV). The combined framework is referred to as the *selective checking and trusted environment (SCATE)* system.

Contributions of this paper:

- we present a framework, SCATE, that protects cyber-physical systems from attacks that falsify actuation commands. [Sec. II-D]
- we use a combination of game-theoretic analysis and a trusted execution environment to deter attackers, significantly reduce checking overheads and still guarantee the safety and integrity of the CPS. [Sec. IV]

We implemented SCATE [Sec. V] on a commercially available ARM Cortex A53 platform [19] and commodity TEE (TrustZone [14]) running embedded Linux. Our system and techniques were evaluated using *four realistic, standardized, cyber-physical systems* [Sec. V-B]: (a) an autonomous ground rover, (b) a flight controller, (c) a robotic arm (typically found in manufacturing systems) and (d) a syringe pump used in medical devices. We also carried out a broader design space exploration [Sec. V-C] using simulated workloads and also analyzed the trade-offs between security and timing/safety properties. Not only does SCATE deter attacks, it is able to do so with significantly fewer overheads and also *guarantee* that it will not compromise the system safety and timing properties. Our open-sourced implementation is available in a public repository [20].

II. MOTIVATION, OVERVIEW AND BACKGROUND

A. The Requirement for Checking Actuation Commands

Real-time CPS consists of *cyber* components and *physical* components. The cyber units perform the computations for estimating the system state (*e.g.*, current location of an unmanned vehicle and the intended direction of its movement) and generation of appropriate control signals for the actuators. The physical components include the entities that are (i) closer to the physical system such as sensors that take measurements and (ii) the actuators that move the physical system.

In a non-secure system, when a task generates an actuation command, it is directly issued to the physical actuators. Figure 1 illustrates this: when a controller task generates an actuation command (say, to set the speed of the motor), the speed is

²Note that the actions taken when we detect a problematic actuation command is orthogonal to the work presented here and depends on the specific CPS. We briefly discuss some of these strategies in Sec. VI.

³This does not preclude the use of other TEEs, *e.g.*, Intel SGX [15].

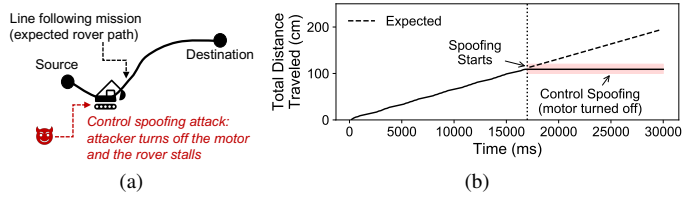


Fig. 2. Illustration of control spoofing attacks on a rover platform: (a) high-level schematic of our experiment setup where a rover performs a line following mission and an adversary triggers malicious code that turns off one of the rover motors; (b) readings from rover motor encoders under control spoofing attack. Without proper control checking, an adversary can inject erroneous signals (shaded region in Fig. 2b) and deviate the rover from its expected behavior (dashed line). In this setup the rover stalled in the middle of its mission due to control spoofing attack as shown by the constant readings from wheel motors).

changed without checking whether the provided speed value is legitimate or not. Without explicit control and verification over the actuation process, it is possible to send arbitrary signals to the actuators and an adversary can drive the system in undesirable ways. For instance, consider ground rovers that can be used in multiple cyber-physical applications such as remote surveillance, agriculture and manufacturing [21]. For demonstration purposes, we use a COTS-based ground rover running an embedded variant of Linux on an ARM Cortex-A53 platform (Raspberry Pi [19]). The rover is equipped with two optical encoders that are connected to the motors (*i.e.*, actuator in this setup); it can turn left by switching off the right encoder and vice-versa.

As depicted in Fig. 2a, we carried-out a line-following mission where the rover steered from an initial location to a target location by following a line. A controller task runs the standard, pre-packaged, proportional–integral–derivative (PID) closed-loop control [22]. A 5-byte value is sent to the actuator (via memory-mapped registers) to control the wheel motors via the I2C interface [23]. This aids in the navigation and control of the rover. The x-axis of Fig. 2 shows the time and the y-axis is the total distance traveled by the rover (*i.e.*, readings from the wheel motors). Since the vendor implementation of the controller does not verify control commands, we were able to inject a logic bomb and send spoofed commands to turn off the motor (at the location marked in the figure). As a result, the rover deviates from its mission. The dashed line (after $t = 17$ seconds) shows the expected behavior (*viz.*, without any attack) as a reference (obtained by running a linear regression test from the traces of an uncompromised execution). As the shaded region in the figure shows, the encoder readings (*i.e.*, traversed distance) remain the same and the rover was not following the line after the attack.

We note that designing and scheduling checking techniques for real-time cyber-physical platforms is often more challenging when compared to the general-purpose systems due to additional timing/safety constraints imposed by such systems (see Table II for related examples). To the best of our knowledge, there is no existing technique that can be directly retrofitted to solve this problem. We believe there is a practical requirement and intellectual merit for designing a framework that can protect actuators in real-time CPS and hence is the focus of this research.

B. System Model

We consider a set of priority-driven, periodic real-time tasks, Γ , running on a multicore CPS platform Π . The set of tasks $\Gamma_p \subset \Gamma$ running on a given core $\pi_p \in \Pi$ is fixed and given by the designers. Each task τ_i issues N_i number of actuation requests. We assume that there is a designer-given quality-of-service (QoS) requirement that $N_i^{min} \leq N_i$ actuation requests (among total N_i number of requests) must be checked (by the trusted entity running inside TEE) for each invocation of a task. We further assume that each actuation command a_i^j is associated a designer-provided weight ω_i^j that represents the importance/preference of checking the corresponding command over other. A higher weight implies that the actuation request is more critical and designers want to examine it more often. We provide a formal representation of our task and real-time model in Appendix A.

C. Adversary Model

Our assumptions on adversarial capabilities is similar to that considered in prior work [24], [25]. In particular, we assume that an adversary can tamper with the existing control logic to manipulate actuation commands, thus modifying the behavior of a system in undesirable ways (*i.e.*, threaten the safety of the system). We only consider the cases where an adversary's actions results in the modification of actuation commands. Other classes of attacks such as scheduler side-channel attacks [26], [27], timing anomalies [24], [28] and network-level man-in-the-middle attacks [29], [30] are not within the scope of this work. However, we do discuss how our approach can be extended to other use-cases and mitigate some of those attacks (Sec. VI). We do not make any assumptions as to how an adversary compromises tasks or actuation commands. For instance, bad software engineering practices leave vulnerabilities in the systems [31]. When the system is developed using a multi-vendor model [32] (where various components are manufactured and integrated by different vendors) malicious code may be injected (say by a less-trusted vendor) during deployment. The adversary may also induce end-users to download modified source code and/or

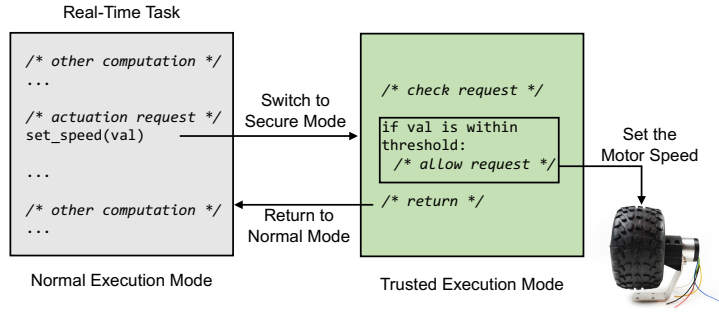


Fig. 3. Flow of operation in SCATE. When a task generates any actuation command, it will be checked by a trusted entity leveraging TEE technologies (say ARM TrustZone [14]). In this illustration the speed of the actuators (motors attached to the wheels) is only set if the speed value is within a predefined range.

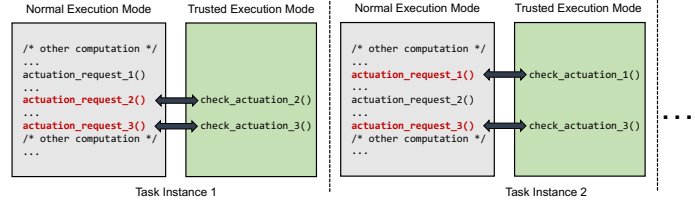


Fig. 4. Random selection of actuation commands for checking.

remote access Trojans, say by using social engineering tactics [33]. We note that embedded real-time CPS have fewer resources and lesser security protections and hence make some of the attacks easier for the adversary [24], [26], [34], [35]. We do not consider the adversarial cases that require physical access, *i.e.*, the attacker can not physically control/turn off/damage the actuators or the system.

D. Problem Overview and Our Approach

Actuation commands that are malicious can jeopardize the safety and integrity of cyber-physical applications. In this research we propose techniques to *protect systems from control spoofing attacks by examining actuation commands before* they are issued to physical peripherals. We name our mechanism, SCATE (selective checking and trusted execution) where we consider cyber-physical applications consisting of software tasks that can have two different types of execution sections: (a) regular (potentially untrusted) execution section where normal executions are carried-out and (b) trusted sections where critical information (*i.e.*, actuation events) are examined.

The high-level schematic of SCATE is depicted in Fig. 3. When a task issues an actuation command, SCATE transfers the control to the secure mode using the TrustZone secure call (SMC) instructions [14]. In the secure mode a designer-provided trusted entity checks the actuation commands. In this work we assume that our checking module uses policy rules that defines the mapping of various system states to corresponding legitimate actuation events (refer to Sec. III for details). We note that although we use ARM TrustZone as the underlying TEE to demonstrate our ideas, other trusted environments can be used in SCATE without loss of generality.

As we shall see in Sec. III-A, the context switch overhead for switching between normal and trusted modes is not negligible. For example, consider the rover used in our experiments (Sec. V and Table II). The execution frequency⁴ of the controller task is 5 Hz (200 ms) and it generates four actuation commands (to set the speeds and direction of attached motors). The controller task must complete execution before its periodic invocation interval (200 ms). If we check the speed and direction values of each of the four commands (using TrustZone), the controller task fails to comply with its timing requirements⁵ (since it requires 261 ms to finish). For such situations (*i.e.*, when not all the commands can be verified without missing timing guarantees for all the tasks), SCATE *selectively checks a subset of the actuation events*. For this, we leverage the tools from *game theory* [16], [17] and randomly select a subset of commands (for checking) that provides us a trade-off between security and timing guarantees (see Sec. IV for details). Figure 4 shows an illustrative case where a task generates three actuation requests and we can check at most two request to comply with timing/safety requirements. In this case SCATE randomly checks two commands each time (*e.g.*, commands [2, 3] in first instance and commands [1, 3] in the second instance). From

⁴Note: these tasks are periodic in nature.

⁵This may cause the rover to deviate from its mission, destabilize or even crash.

the earlier rover example, by reducing the number of checks in half⁶ (e.g., randomly checking two commands in each task instances instead of all four), the controller task in SCATE manages to finish before 200 ms without significantly degrading security as explained in Sec. V.

E. Background

We now provide a background on real-time CPS, the TEE technology (ARM TrustZone [14]) and the game-theoretic modeling [17]) used in our work.

1) *Real-Time Cyber-Physical Systems*: Systems with real-time properties need to function correctly, but *within their predefined timing constraints*, often termed as a “deadlines”. The usefulness of results produced by the system usefulness drops sharply (see Fig. 5). This is different from general-purpose systems where the usefulness drops in a more gradual manner (e.g., a web service may tolerate a few millisecond delays without significantly degrading user experience). For example, consider the CPS use-case of a car’s airbag deployment, where the system must react (i.e., detect the collision and deploy airbags) within 60 ms [36]. If the airbag deployment process fails to respond within its timing constraints (e.g., 60 ms), it can have catastrophic results and threaten the safety of the passengers. Each real-time application in the system (called “task”) represents a time-critical function such as estimating system state/dynamics or issuing requests to physical peripherals. The scheduler in a real-time operating system (RTOS) uses timers and interrupt handlers to enforce timing guarantees (deadlines) at runtime. Some of the common properties and assumptions related to real-time CPS are as follows: (i) implemented as a system of periodic tasks that periodically perform sensing/actuation operations (ii) memory and processing power often limited and (iii) stringent timing and safety requirements.

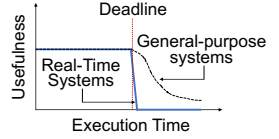


Fig. 5. Timeliness requirements of real-time systems.

2) *ARM TrustZone*: Trusted environments are set of hardware and software-based security extensions where the processors maintain a separated subsystem in addition to the traditional OS (also called rich OS) components. TEE technology has been implemented on commercial hardware such as ARM TrustZone [14] and Intel SGX [15]. In this work we consider TrustZone as the building block of our model due to the wide usage of ARM processors in CPS. We note that although we use the TrustZone functionality for demonstration purposes, our ideas are rather general and can be adapted to other TEE technology without loss of generality.

TrustZone contains two different privilege blocks: (i) regular (non-secure) execution environment, called “Normal World” (NW) and (ii) a trusted environment, referred to as “Secure World” (SW). The NW is the untrusted environment that runs a commodity untrusted OS (called rich OS) whereas SW is a protected computing block that only runs privileged instructions. TrustZone hardware ensures that the resources in the SW can not be accessed from the NW. These two worlds are bridged via a software module, the *secure monitor*. The context switch between the NW and SW is performed via a *secure monitor call* (SMC).

3) *Normal-Form Games*: The overheads for TEE context switch is costly (Sec. III-A). *If a task cannot verify all the actuation commands, we propose to select only a subset of commands in each job* for checking. For this, we leverage the tools from game theory [37] to ensure that the chosen subsets are non-deterministic, at least from the adversary’s point of view (see Sec. IV for details). In multi-agent systems, if the optimal action for one agent depends on the actions that the other agents take, game theory is used to analyze how an agent should behave in such settings. In a *normal-form game* [17], every player $j \in \{1, 2, \dots, J\}$ has a set of strategies (or actions) σ_j and a utility function $u_j : \sigma_1 \times \sigma_2 \times \dots \times \sigma_J \rightarrow \mathbb{R}$ that maps every outcome (a vector consisting of a strategy for every player) to a real number. As we shall see in Sec. IV-A we formulate our problem as a *two-player game* (e.g., system designer and adversary). The output of the game finds the probability distribution over the player’s strategies (i.e., fraction of time a given strategy is selected in the game) that leads to optimal outcome. While game-theoretic analysis has been used in other modeling problems (e.g., patrolling [18], network routing [38], transportation systems [39]) as well as general-purpose control systems/CPS [40]–[43], they are not real-time aware and do not consider the problem of protecting physical actuators. To the best of our knowledge this is the first work that uses normal-form games in the real-time security context.

III. CHECKING ACTUATION COMMANDS

In SCATE, a “checking module” executes inside the trusted environment. The checking module observes system states and decides whether a given actuation command is legitimate or malicious. Recall that when a task issues actuation requests, we transfer control to the secure execution mode using TrustZone SMC instructions. In particular, for a given real-time platform we assume that there exists a $\text{CheckAct}(\tau_i, a_i^j, t)$ function⁷ that examines a given actuation command a_i^j (where $1 \leq j \leq N_i$, N_i is total number of commands the task issues) generated by a task τ_i at a given time t . As shown in Fig. 6a, the checking

⁶Section V presents details of this experimental setup and additional results.

⁷The exact function depends on the specific CPS and application requirements.

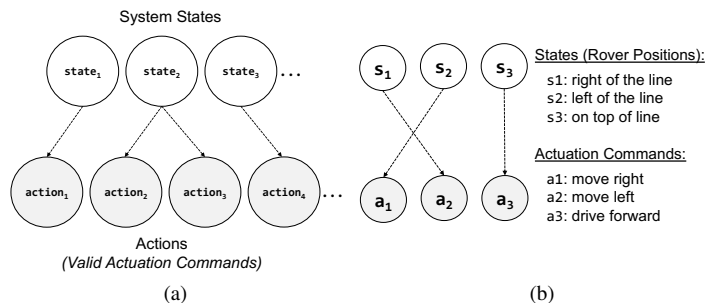


Fig. 6. (a) $State \rightarrow Action$ mapping used in SCATE for checking actuation commands. (b) Example states and corresponding valid actuation commands for a line-following rover.

module uses policy abstraction rules [44], *viz.*, $State \rightarrow Action$ pairs where the $State$ predicate represents a given system state and $Action$ denotes corresponding valid actuation command(s). In particular, we assume that when τ_i executes an actuation command, function $CheckAct(\tau_i, a_i^j, t)$ first observes the system state $\mathcal{S}(t)$ and then decides whether the actuation command a_i^j is valid for the current state $\mathcal{S}(t)$.

Consider the line-following rover presented in Sec. II-A. The directions for the wheels of the rover (*i.e.*, forward, left and right; controlled by the attached motors) are the actuation commands. At any given point in time, the rover can be in one of three states: $\mathcal{S} = \{ON_LINE, LEFT_OF_LINE, RIGHT_OF_LINE\}$ that denotes whether the rover is on top of the line or shifted left/right of the line, respectively. The rover controller task performs the following actuation operations (*i.e.*, actions): `move_left()/move_right()` (move the rover left/right, respectively) and `move_forward()` (drive the rover forward). The corresponding $State \rightarrow Action$ mapping for this rover is illustrated in Fig. 6b. If the rover is on the left side of the line (*i.e.*, $State = LEFT_OF_LINE$), the valid command should be `move_right()` (*i.e.*, shift the rover back so that it stays on the line) and if the rover is on top the line (*i.e.*, $State = ON_LINE$), the controller task should drive it forward (*i.e.*, issue `move_forward()` command).

Table VII in the Appendix B summarizes the possible checks for various real-time platforms — however, this is by no stretch meant to an exhaustive list. We assume that $State \rightarrow Action$ rules are given by the designers based on system requirements. We note that the ideas presented here are agnostic to the specific checking method and SCATE is compatible with existing techniques (*e.g.*, defining rules at design times [25], [45], deriving from specifications [46] and based on statistical analysis [47]). In this work we focus on how to selectively examine random subsets of actuation commands by using such designer-provided checking rules. In Sec. V-B we describe the implementation of `CheckAct()` functions for four realistic platforms used in our evaluation.

A. The Requirement for Coarse-Grain Checking

In order to check actuation commands we must ensure that SCATE should not cause inordinate delays and the timing requirements of real-time tasks are satisfied (*i.e.*, they complete execution before their respective deadlines). We therefore develop design-time tests (see Appendix C) that ensure tasks meet their timing requirements (deadlines). Our analysis in Appendix C shows that there is an overhead for inspecting the actuation commands using TEEs and a task may miss its timing/safety requirements as a result. As we mentioned earlier, any failure to meet timing requirements disrupts the stability of the system and can be catastrophic. For instance, consider the rover example from Sec. II-D. If the controller task fails to issue navigation commands before the time limit, the rover may stall, or worse, may not be able to steer properly and even crash. Hence, delays caused by the checking mechanisms can also cause such problems. Table II presents additional examples for the possible consequences when tasks are unable to meet their timing requirements.

Existing work [48]–[50] shows that although TEEs are implemented on hardware, they can still cause significant overheads — this is particularly acute in real-time applications. For instance, consider the Linux-based TrustZone port, OP-TEE [51] supported on many embedded platforms. Our experiments show that the overhead of switching between normal to trusted mode is around 66 ms for OP-TEE on a Raspberry Pi platform. For completeness, we also performed experiments on an ARMv8-M Cortex-M33 architecture using ARM FVP libraries [52] where the regular applications were running on FreeRTOS [53] and trusted mode codes were executed on bare-metal. We find that the mode switching delays in this setup are 2 ms. We note that the delays are higher in the Linux environment due to extra overheads (*i.e.*, execution of sequence of API calls [48]) imposed by the Linux kernel and OP-TEE secure OS. Although the overheads of secure calls (SMC) for switching between regular and trusted modes are platform-specific, it may still not be feasible to check multiple commands while meeting real-time guarantees. For example, if a task operates at 50 Hz (*i.e.*, it is required to finish before 20 ms) [26] and regular computation takes 10 ms, the FreeRTOS-based setup allows at most 5 checks in order to comply with timing requirements. Likewise, for

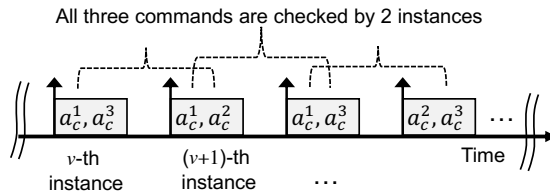


Fig. 7. Non-deterministic checking: *all* commands are eventually checked.

the applications running on a Linux and OP-TEE-based Raspberry Pi platform⁸ (Sec. V-B), we can check at most 3 commands per instance if the controller task operates at 5 Hz. We therefore need smart techniques, say where *only a subset of commands are vetted* while maintaining security guarantees, to support both security and performance for real-time applications. We now present my methods to achieve this (based on game-theoretic analysis) in the following section.

IV. GAME-THEORETIC ANALYSIS FOR SMART ACTUATION CHECKS IN SCATE

We now propose a mechanism to deal with this issue of monitoring overheads. We consider the case when there exists a task τ_i such that it cannot perform all the N_i checks before its deadline (denoted by D_i). One option to reduce the number of checks is to verify only a subset of commands so that the task can finish before its deadline. That is, check a subset of commands, K_i , ($N_i^{min} \leq K_i < N_i$) such that $R_i^{TEE} \leq D_i, \forall \tau_i \in \Gamma$ where R_i^{TEE} is the response time (*i.e.*, time between task arrival to completion, used to verify that the task meets its deadline [54]). The challenge is then to decide *which* subset of K_i (among N_i) actuation requests should be selected for checking in each task τ_i . In addition, if we check only a fixed set of K_i commands and an adversary jeopardizes some or all of the remaining $N_i - K_i$ requests, then the attack will succeed and remain undetected. To balance the security and real-time requirements, SCATE *randomly selects different subsets of requests for checking*. In particular, during each task execution we randomly pick a set of K_i commands with pre-computed probability distributions. While we pick a subset of commands, it should look like (to adversary) that SCATE *is checking all commands*. As a result, it will be difficult for an attacker to identify which subset of requests are selected for checking since each instance of a task will select a different subset of requests for vetting. As we shall see in Sec. IV-A we formulate this problem as a two-player game [17] and develop Algorithm 1 to determine the feasible number of K_i inspection points that provide similar level of security when compared to the case that checks all N_i requests. We now illustrate our ideas used in SCATE with a simple example.

Intuition and Example. Let us consider a ground rover performing a line-following mission. The rover controller task (τ_c) generates the following actuation requests ($N_c = 3$): (a) `setEncL(val)` and `setEncR(val)` that set the speed of left and right motor encoders, respectively (denoted by a_c^1 and a_c^2); (b) `setNav(cmd)` that issues a navigation command where each *cmd* specifies values to the peripheral registers for navigating the rover forward, backward, left or right directions (denoted by a_c^3). Recall from the description of the system model that there exists designer-provided weights ω_i^j for checking each of the commands a_i^j (see Appendix A) and that is given by: $\Omega_c = \{\omega_c^1, \omega_c^2, \omega_c^3\}$. As we shall see in Sec. IV-A, the weights are used to determine which commands should be checked more often. For example, if $\omega_c^2 = 2$ and $\omega_c^1 = \omega_c^3 = 1$, then SCATE tends to check `setEncR(val)` twice as often as the other two commands. The checking for a_c^1 and a_c^2 is whether the speed value is within a given bound (*e.g.*, $val \in [v^-, v^+]$) and for a_c^3 the checking module verifies if the *cmd* value is consistent so that the rover is on the line and is correctly following the mission.

We now consider the case when checking all three requests does not comply with the timing requirement of task τ_c and we can only verify at most $K_i = 2$ requests (we describe how to calculate the value of K_i for each task τ_i in Sec. IV-B). Therefore, the possible combinations for checking are as follows: $X_c = \{(a_c^1, a_c^2), (a_c^2, a_c^3), (a_c^1, a_c^3)\}$. In SCATE, for each instance of the task τ_c we randomly select any j -th element from the set X_c with probability x_c^j that provides better “monitoring coverage”. For example, let $x_c^1 = x_c^2 = 0.25$ and $x_c^3 = 0.5$. Then, for any given instance of τ_c the possibility of verifying both a_c^1 and a_c^2 is 25%, verifying both a_c^2 and a_c^3 is 25%, where the possibility of verifying a_c^1 and a_c^3 is 50% (recall that by assumption we can check only 2 commands per job). Figure 7 presents an instance of such execution. SCATE ensures that although we pick a subset of commands each time, eventually *all* the commands are checked. For example, in Fig. 7 SCATE requires two instances to check all three commands. In the following section we present our ideas to compute these probabilities using game-theoretic analysis.

A. Generating Randomized Schedules

We now present our techniques to derive the probabilities for selecting subsets of commands to be checked. The formulations in this section assumes that the size of feasible subset of K_i commands, that ensures all timing requirements are met, is known

⁸We implemented SCATE using OP-TEE/Linux-based Raspberry Pi platform to support multiple off-the-shelf systems.

System Reward:

$$\lambda_i^{j,l} = \frac{\sum_{w \in \Psi(X_i^j)} w}{\sum_{w \in \Psi(X_i^j) \cup \Psi(Q_i^l)} w}, \quad (1)$$

normalization factor: union of designer's and adversary's strategies

System Cost:

$$\zeta_i^{j,l} = \frac{\sum_{w \in \Psi(Q_i^l)} w}{\sum_{w \in \Psi(X_i^j) \cup \Psi(Q_i^l)} w}, \quad (2)$$

normalization factor: union of designer's and adversary's strategies

Fig. 8. Reward and cost functions.

for each task. In Sec. IV-B we present algorithms to derive K_i . We model the selection of a subset of commands (for checking) as a *two-player normal-form game* (also called leader-follower game) [16]–[18]. The game formulations allow the designers to model the fact that an attacker acts with knowledge of the defender's actions and react accordingly. Since normal-form games address the challenges posed in our context (*i.e.*, selecting optimal actions for decision-making agents), we use this game model in SCATE for generating randomized schedules.

1) *Game Setup:* In our model we consider two players: The leader (*i.e.*, system designers) and the follower (*i.e.*, adversary). Let X_i denote the set of all combinations of choosing K_i subset of commands from total N_i number of possibilities, *i.e.*, the size of set $|X_i| = \binom{N_i}{K_i} = \frac{N_i!}{K_i!(N_i-K_i)!}$. In game-theoretic terminology X_i represents the set of leader's "strategies". As discussed in the previous section, the j -th element of X_i is a vector of size K_i that represents which subset of commands will be picked for inspection in the secure enclave. Let us now introduce the variable Q_i that represents the attacker's set of actions (*i.e.*, follower's strategies). The set Q_i represents the possible combinations of actuation requests invoked by task τ_i that can be compromised by an adversary. Recall from the rover example where the controller task τ_c invokes $N_c = 3$ actuation requests, hence, the adversary can pick one of the following eight combinations: $Q_c = \{(a_c^1), (a_c^2), (a_c^3), (a_c^1, a_c^2), (a_c^2, a_c^3), (a_c^1, a_c^3), (a_c^1, a_c^2, a_c^3), (\emptyset)\}$. For example, the first element in the set denotes the adversary chooses to compromise only invocation a_c^1 , the fifth element implies both a_c^2 and a_c^3 are compromised while the last element implies there is no attack during this instance of the task. Note that the size of the attacker's strategy set Q_i is 2^{N_i} .

Recall that each actuation command a_i^j is associated with a designer-given weight ω_i^j (see Sec. II-B and Appendix A). A higher weight implies that designers want to check the corresponding command more often. For instance, from the rover example, designers may want to check navigation commands (a_c^3) more frequently than the ones that set the wheel speeds (a_c^1, a_c^2) and may set higher weight for ω_c^3 . Let $\Lambda(X_i^j)$ denote the set of commands used for vetting and $\Psi(X_i^j)$ is the set of corresponding weights in the j -th element of the strategy set X_i . Likewise $\Lambda(Q_i^l)$ denotes the set of commands and $\Psi(Q_i^l)$ is the corresponding set of weights compromised by the attacker in its l -th strategy. In the rover example, if we select $j = 2$ and $l = 4$ (*i.e.*, second and fourth elements of the designers and adversary's strategy set) then $\Lambda(X_c^2) = \{a_c^2, a_c^3\}$, $\Psi(X_c^2) = \{\omega_c^2, \omega_c^3\}$ and $\Lambda(Q_c^4) = \{a_c^1, a_c^2\}$, $\Psi(Q_c^4) = \{\omega_c^1, \omega_c^2\}$.

We now introduce two variables, *viz.*, *system reward* (λ) and *system cost* (ζ). A *higher system reward and lower cost is good for the designers and bad for the attackers*. Likewise, higher system cost and lower reward is favorable for the adversary's point of view (and bad for the designers). If a task τ_i selects the j -th element from the set of strategies X_i and the attacker selects the l -th strategy from Q_i for attack then the system reward is $\lambda_i^{j,l}$ and cost is $\zeta_i^{j,l}$. If the task selects a subset of commands for vetting in its j -th strategy and the adversary also attacks those invocations in its l -th strategy, *i.e.*, $\Lambda(X_i^j) = \Lambda(Q_i^l)$, it implies that the attack is detected. Hence, we set $\lambda_i^{j,l}$ to a large positive value (*i.e.*, high system reward, since the attack is detected) and $\zeta_i^{j,l}$ a large negative value (*i.e.*, no system cost). In contrast, if $\Lambda(X_i^j) \cap \Lambda(Q_i^l) = \emptyset$ for any pair (j, l) , *i.e.*, $\Lambda(X_i^j)$ does not contain any commands in attackers l -th strategy $\Lambda(Q_i^l)$, that implies the compromised commands are not vetted (*i.e.*, the spoofed command is not checked). In this case we set $\lambda_i^{j,l}$ a large negative value (*i.e.*, no reward) and $\zeta_i^{j,l}$ a large positive value (*i.e.*, high system cost). When the above two conditions do not hold (*i.e.*, only a subset of the compromised commands are

Algorithm 1 SCATE: Parameter Selection

Input: Input taskset parameters Γ **Output:** For each task τ_i , the size of the feasible set $K_i^* \geq N_i^{min}$ and selection probability $x_i^j, j = 1, \dots, |X_i^*|$ for each of the combinations in the strategy set X_i^* ; Infeasible otherwise.

```
1: /* Check minimum feasibility requirements */
2: for each  $\tau_i \in \Gamma$  do
3:   Set  $K_i = N_i^{min}$  and calculate response time  $R_i^{TEE}$  using Eq. (3)
4: end for
5: /* Unable to integrate SCATE with minimum QoS requirements */
6: if  $\exists \tau_i$  such that  $R_i^{TEE} > D_i$  then
7:   return Infeasible
8: end if
9: for each task  $\tau_i$  (from higher to lower priority order) do
10:  Find maximum  $K_i^* \in [N_i^{min}, N_i]$  such that all low-priority tasks  $\tau_l$  meet their timing requirements (i.e.,  $R_l^{TEE} \leq D_l$ )
11:  /* not all the commands can be examined – obtain parameters for non-deterministic checking */
12:  if  $K_i^* < N_i$  then
13:    Determine the strategy set  $X_i^*$  for  $K_i^*$  where  $|X_i^*| = \binom{N_i}{K_i^*}$  and obtain probabilities  $x_i^j$  by solving the game formulation
14:  end if
15:  Update response time  $R_l^{TEE}$  for each  $\tau_l$  that executes with a priority lower than  $\tau_i$  with the updated size  $K_i^*$ 
16: end for
17: /* return the solution */
18: return the size of the feasible set  $K_i^*$  and probability  $x_i^j$  of selecting  $j$ -th strategy ( $j = 1, 2, \dots, |X_i^*|$ ) from  $X_i^*$  for each task  $\tau_i \in \Gamma$ 
```

checked) and therefore $\exists(j, l)$ such that $\Lambda(X_i^j) \cap \Lambda(Q_l^i) \neq \emptyset$, we then obtain the system reward/cost by *normalizing the weights* of both adversary and designer's strategies. For this, we define the reward and cost functions in Eq. (1) and Eq. (2), respectively (see Fig. 8). Let us revisit the rover example with $j = 2$ and $l = 4$. In this case $\lambda_c^{2,4} = \frac{\omega_c^2 + \omega_c^3}{\omega_c^1 + \omega_c^2 + \omega_c^3}$ and $\zeta_c^{2,4} = \frac{\omega_c^1 + \omega_c^2}{\omega_c^1 + \omega_c^2 + \omega_c^3}$.

This reward and cost functions give us one way to measure the security of the system in terms of how many significant actuation commands we can monitor given an attacker's strategy. A higher system reward (and lower cost) implies that SCATE performs more checking with respect to a given adversarial action.

2) *Formulation as an Optimization Problem:* We now develop models to determine the optimal strategy for each of the tasks. Let us now denote x_i^j as the probability of selecting the j -th element from X_i (represents the proportion of times in which a strategy j is used by the task τ_i in the game). The output of the game will provide the probability distribution of (randomly) selecting subset of K_i commands from the set possible choices (i.e., X_i) for the different execution instances of a given task τ_i . For a given adversarial strategy l , summing over all the strategy sets X_i (i.e., $\sum_{j=1}^{|X_i|} x_i^j \lambda_i^{j,l}$ and $\sum_{j=1}^{|X_i|} x_i^j \zeta_i^{j,l}$) gives us the total system reward and cost, respectively.

We can obtain probability distributions of selecting elements from X_i for a given attacker strategy l (that maximizes the system reward) by forming a linear optimization program. In particular, for each of the attacker's l -th strategy (where $1 \leq l \leq |Q_i|$), we compute a strategy for the τ_i such that (i) playing l -th strategy is a best response from the adversary's point of view (i.e., more system cost) and (ii) under this constraint, the strategy maximizes the reward for τ_i (i.e., checks critical commands more often). Appendix D presents the details of our linear programming formulation.

B. Calculating the Size of the Feasible Command Set

Our focus here is to *examine as many actuation commands as possible* while meeting real-time guarantees. The game formulation from the previous sections assumes that we know the size of the set K_i and calculate the probabilities accordingly. However, in a system with multiple real-time tasks, finding the size of feasible set K_i for each task $\tau_i \in \Gamma$ while also meeting the real-time requirements (deadlines) is a non-trivial problem. We therefore develop an iterative solution for finding the size of this set.

Our proposed solution works as follows (refer to Algorithm 1 for a formal description). In Lines 1–4, we first assign $K_i = N_i^{min}, \forall \tau_i$ and check whether all tasks meet their timing requirements (i.e., finish before their deadlines). If there exists a task that fails to meet its timing requirements, we report that it is “*infeasible*” to integrate SCATE in the target system while still satisfying designer specified QoS requirements (Line 7). This infeasibility result provides hints to the designers to either update or modify system parameters (e.g., number of commands, QoS requirements) to enable the ability to check actuation commands in the system. Otherwise, we optimize the number of commands a task can verify in an iterative manner (Lines 9–16). To be specific, for a given task τ_s we perform a logarithmic search (see Algorithm 2 in Appendix E for the pseudo-code) and find the maximum number of commands K_i^* that can be verified within the range $[N_i^{min}, N_i]$ such that all low-priority tasks τ_l meets their timing requirements with actuation checks enabled (Line 10). If the selected parameter K_i^* is less than the total commands N_i , we then use game theoretical-analysis from Sec. IV-A and obtain probabilities of randomly selecting K_i^* commands (in each task instance) from a total of N_i commands (Line 13). The above process is repeated for all the tasks.

TABLE I
SUMMARY OF OUR IMPLEMENTATION PLATFORM

Artifact	Configuration
Platform	Broadcom BCM2837 (Raspberry Pi 3)
CPU	1.2 GHz 64-bit ARM Cortex-A53
Memory	1 Gigabyte
Operating System	Linux (NW), OP-TEE (SW)
Kernel version	Linux kernel 4.16.56, OP-TEE core 3.4
Interface	I2C
Boot parameters	dtparam=i2c_arm=on, dtparam=spi=on, force_turbo=1, arm_freq=1200, arm_freq_min=1200, arm_freq_max=1200

V. EVALUATION

In this section we first present our implementation details (Sec. V-A). We then show the viability of SCATE using (i) four realistic cyber-physical case-studies (Sec. V-B) and (ii) simulated workloads for a broader design-space exploration (Sec. V-C).

A. Implementation

We implemented SCATE on Raspberry Pi 3 Model B [19] (equipped with 1.2 GHz 64-bit ARMv8 CPU and 1 GB RAM). We selected Raspberry Pi as our implementation platform since (a) it is a COTS system that supports a commodity TEE (ARM TrustZone), (b) existing literature has shown the feasibility of deploying cyber-physical applications on Raspberry Pi [25], [33], [55]–[58] and (c) it provides a robust development environment that allows us to analyze the viability of our approach for multiple realistic off-the-shelf cyber-physical systems on a common platform. In our experiments we considered both, motors (DC as well as stepper) and servos as actuators. We used the Adafruit motor shield [59] (an I/O extension daughter-board for Raspberry Pi) that allowed us to control multiple actuators using the I2C interface. We used an open-source motor driver [60] and servo controllers [61]. We implemented the trusted execution modes using the OP-TEE [51] software stack that uses GlobalPlatform TEE APIs [62]. OP-TEE provides a minimal secure kernel (called OP-TEE core) that can be run in parallel with a rich OS (e.g., Linux). We used an Ubuntu 18.04 filesystem with a 64-bit Linux kernel (version 4.16.56) as the rich OS and executed our CheckAct() functions in the OP-TEE secure kernel (version 3.4). Our controller and checker codes are written in C for compatibility with the OP-TEE APIs. For accuracy of our measurements we disabled all the frequency scaling features in the kernel and executed RP3 at a constant frequency (i.e., 1.2 GHz, the maximum supported clock speed). This was to ensure that values observed in different trials and case-studies were consistent.





We solved the linear programs using the Python-MIP library [63] with CBC solver [64]. From the probabilities obtained by the game model (Sec. IV-A), at runtime (i.e., for each instance of a task) we used the roulette-wheel selection technique [65] and a standard C random number generator for selecting a random subset of commands. However, this does not preclude the use of other hardware-supported generators such as ZIFFER [66] and OneRNG [67] to ensure tamper-proof true random number generation that will further improve the security of SCATE. For each of the selected commands, control was transferred to the secure enclave (i.e., OP-TEE core) for the checking. For each of our case-studies, we implemented the CheckAct() functions as OP-TEE trusted applications. The implementation and details of CheckAct() for the each of platforms are presented in Sec. V-B. We note that our implementation using Raspberry Pi, Linux and OP-TEE serves as a good proof-of-concept and can be extended with other OS, hardware platforms and TEE architectures without loss of generality. Our implementation code is available in a public repository [20]. Table I summarizes the system configurations and implementation details.

B. Experiments with Realistic Cyber-Physical Platforms

We chose four realistic real-time cyber-physical platforms as case-studies to evaluate the efficacy of SCATE: (a) ground rover, (b) UAV flight controller, (c) robotic arm and (d) syringe/infusion pump that are used in many cyber-physical applications. These are *off-the-shelf platforms and we did not modify them*. Table II summarizes the properties of each of these systems and attack/detection techniques used in our experiments. We note that unlike generic applications, there are few publicly available open-source real-time platforms due to their proprietary nature (see more in Sec. VI). In addition, there is a significant amount of effort involved in setting up a TEE-supported real-time cyber-physical platform and generating evaluation traces from it. We therefore limit ourselves to four real-time platforms in this paper — albeit they cover a wide range of application domains (see Table VII) and should suffice to demonstrate the feasibility of our approach.

Since we focus on scheduling independent actuation checking events, the type of attacks and checking techniques are orthogonal to our model. For demonstration purposes, we use fault injection [68], [69] to mimic malicious behavior and trigger attacks that are known to the checking module (i.e., CheckAct() function). Note that this is a standard technique used by the researchers to evaluate security solutions in cyber-physical applications [6], [21], [25], [35], [68], [70]. We now present the evaluation platforms used in our experiments.

TABLE II
REAL-TIME CYBER-PHYSICAL PLATFORMS USED IN OUR EXPERIMENTS

Platform	Application	Real-Time/Safety Requirements	Actuation Commands	Attack Demonstration	Checks inside Enclave
	The rover performs a line following mission. The controller task sets the speed of the rover and steers the wheels (based on its position on the line) by executing a PID control loop	Set the speed and direction of the motors for the wheel movements within sampling interval (<i>i.e.</i> , control loop frequency, set at 5 Hz)	<ul style="list-style-type: none"> Set the speed of the wheels Set wheel directions (left, right, forward and backward) 	DoS attack [25]: arbitrarily sets high speed for one of the wheel motors	The speed of motors can only be within predefined limit
	Executes a PID control loop and issues PWM signals to four motors connected to the four propellers of a quad-copter	Issue the PWM signal within sampling frequency interval (5 Hz in our setup) to ensure the quad-copter is stable	<ul style="list-style-type: none"> Set PWM frequency Set PWM pulse duration (four, one for each of the propellers) 	Parameter corruption attack [35]: modify PID control coefficients and send incorrect PWM pulse to the front right motor	Check PID control coefficients (<i>i.e.</i> , pulse duration values) before issuing PWM signals to the motos
	The robot arm performs the following operations in a sequence: pick an object (close it claws), move the arm to destination position, drop the object (open claws) and reset the arm back to initial position	Complete movement of the object before arrival of the next object; inter-arrival duration of the objects was set at 250 ms	Set rotation angle for each of the four servos	Synchronization attack [68]: sends incorrect <code>angle</code> value to the servo channel and prevents the arm from resetting back to its initial position	Check the consistency of each (<code>channel</code> , <code>angle</code>) pair (<i>i.e.</i> , the <code>angle</code> value for a given servo <code>channel</code> can not be more than the designer provided bounds) before issuing pulses to the servo motors
	The pump pushes certain amount of fluid and then pulls the trigger to reset the syringe to its initial position	Perform the push/pull operations within designer specified time limit (set at 300 ms)	<ul style="list-style-type: none"> Set motor rotation frequency Drive the motor forward/backward to push the fluids and reset the motor position 	Bolus tampering attack [55], [68]: the attacker injects more fluid than the permitted volume	Checks the amount of fluid the motors can pump (<i>i.e.</i> , monitor the number of PUSH/PULL events the controller task invokes)

• **Case-Study #1 (Ground Rover):** Our first case-study platform is the ground rover introduced in Sec. II-D. There are two motors attached to the rover wheels (the actuators in our context). We used an open-source implementation of the rover controller (written in Python) [71] and ported it to C for compatibility with OP-TEE APIs. The rover performed a line-following mission where it moved from a source to a target way-point by following a line. Each instance of the controller task first set the speed of the motor for the wheel movements and then steered (*e.g.*, forward, left or right) based on its position on the line. **Actuation:** The rover has four actuation commands: two for setting the speed of both of the wheels and two for issuing navigation commands to the two motors attached to the wheel. Table II lists these actuation commands.

Attack and Consequences: We injected a DoS attack [25] that arbitrarily sets a high speed for one of the motors (to destabilize the rover and move it away from the line). This attack can deviate the rover from its way-points (or even crash it) due to the imbalance in the wheel speeds.

Detection: In our setup the `CheckAct()` functions validate whether the rover speed is within designer-given predefined thresholds [72] and also verifies whether the navigation commands were consistent with the rover position. We detected the DoS attack by checking the bounds on the speed (*i.e.*, 70–100 decimal values [72]) issued by the controller task.

• **Case-Study #2 (Flight Controller):** Our second case-study is a flight-controller for a quad-copter [73]. The original controller code is developed for Arduino platforms. Since Arduino boards do not support TrustZone, we ported it to the Raspberry Pi and OP-TEE enabled environments. In this setup the controller executes a PID control loop using the Ziegler–Nichols method [74] and sends pulse width modulation (PWM) signals to spin each of four motors (*i.e.*, actuators) connected to the propellers.

Actuation: There are five actuation commands: one for setting the PWM frequency and other four are for sending PWM pulse durations for each of the motors to rotate the copter propellers. The `CheckAct()` functions validate whether the PWM frequency and pulse durations sent to each of the motors were within a certain range (obtained from PID control logic).

Attack and Consequences: For this case study we considered a parameter corruption attack [35] that modifies the control parameters (*e.g.*, the PID control coefficients) at runtime and sends incorrect pulse values to the front-right motors. This attack can suddenly turn off/freeze the propellers. As a result, the copter will instantly fall/crash.

Detection: This attack is detected since we verify the PID parameters and corresponding PWM pulse durations.

• **Case-Study #3 (Robotic Arm):** Our next case-study platform is a robotic arm used in manufacturing systems. The movement of the robotic arm is controlled by four servos (actuators in our context). Each servo is connected to a specific “channel” (I/O port) in the Adafruit motor shield. We use an open-source Python-based robot controller [75] and adapted the implementation for our C-based setup.

Actuation: Our robot performed an assembly line sequence with the following four actuation operations: `PICK()`, `MOVE()`, `DROP()` and `RESET()` that (i) picks an object from first position, (ii) moves the arm to a final position, (iii) drops the object

TABLE III
NUMBER OF ACTUATION COMMANDS

Platform	Total Commands (N)	Selected for Vetting ($K = \lfloor 0.5N \rfloor$)
Ground Rover	4	2
Flight Controller	5	2
Robotic Arm	4	2
Syringe Pump	7	3

and, finally, (iv) resets the arm to initial position (to pick up another object). Each operation takes a (channel, angle) pair that controls the rotation of the corresponding servo to the desired angle (45° in our setup [75]).

Attack and Consequences: We used a synchronization attack [68] that destabilizes the assembly line by preventing the robot from resetting its arm back to the initial position. To demonstrate this, we injected a logic bomb that sets an incorrect angle value in the RESET() operation (e.g., servo channel 3). This attack can collapse the whole assembly line since the arm is not returned to the initial position and hence is unable to pick up objects queued in the line.

Detection: CheckAct() detects this attack since it asserts that each servo can only move up to a certain designer provided angle (45°) for each of the operations.

- **Case-Study #4 (Syringe Pump):** Our final case-study platform is a syringe/infusion pump [76]. In our experiments we considered a bolus delivery use-case [55], [77] where the syringe pump first pushes a certain amount of fluid (PUSH event) and then pulls the trigger back (PULL event). The syringe movement is controlled by a stepper motor. Since the original implementation is for Arduino platforms (and does not support TrustZone), we modified the codes to make it compatible with Raspberry Pi and its motor driver library.

Actuation: For a given fluid amount, the syringe pump implementation selects the number of steps where the PUSH and PULL events should be called. We considered each of the PUSH/PULL events as actuation requests since they set the direction of motor rotation. In our setup there were seven actuation requests: one for setting the motor rotation frequency and six for PUSH and PULL events (three each). PULL events were called after all three PUSH operations were completed.

Attack and Consequences: We implemented a bolus tampering attack [55], [68] where the adversary injects more fluid than is required (i.e., more than three PUSH events). The attack has serious safety consequences and is a health hazard since it can inject more fluids/medications to the patient body than the permitted amount.

Detection: This attack is detected by CheckAct() since it verifies the motor frequency and how many times each of the PUSH/PULL events are called.

Experience and Findings. In our study we compare SCATE against a naive scheme that checks *all* the actuation commands. We refer to this latter technique as the “*fine-grain*” checking scheme. Note that in fine-grain checking, there are more context switches between the normal and secure execution modes since *all* the commands are checked. The goal of our evaluation was to *study the trade-offs between security and real-time requirements*. We therefore considered the subset of commands selected for checking were no more than 50% of the total number of commands so that tasks can finish before their timing requirements (see Table II)⁹ (i.e., $K = \lfloor 0.5N \rfloor$) and assumed equal weights for all commands. We note that our implementation is modular and can be easily adjusted with different weight values. Table III lists the total number of commands (N) and subset of commands (K) for each of evaluation platforms. We now discuss the results of applying these schemes on the four case-studies and address the following research questions (RQs):

- **RQ1.** *How quickly an intrusion can be detected by SCATE when compared to the fine-grain scheme?*
- **RQ2.** *What are the performance impacts and runtime overheads of these schemes?*

Security Analysis: In the first set of experiments (Fig. 9) we analyze the delay in detecting the attacks: a comparison between SCATE and fine-grain scheme. The workflow of our experiments for each of the case-studies was as follows: for a given platform and for each of our experiments (x-axis of Fig. 9) we triggered the attack at random points in time (i.e., during the execution of the victim task) and measured the time delay (in terms of number of task instances¹⁰, y-axis in Fig. 9) in the detection of the commands by CheckAct() function. In the fine-grain scheme, the time to detect an attack is upper bounded by the sampling interval (period), T_i (i.e., requires at most one task instance). From our experiments, with 1000 individual trials for each of the four platforms, we found that the mean and 99th-percentile detection delay were 1–3 and 3–12 sampling intervals, respectively (refer to Table IV for exact values). We note that this delay in detection results in improve response time and reduced resource usage (see more in the following experiments) and that could be acceptable for many real-time applications¹¹.

⁹We also carried out additional experiments to show the effect of varying this parameter (see Sec. V-C).

¹⁰If the detection delay is \hat{y} task instances, it implies that SCATE requires $\hat{y}T_c$ additional time units to detect the attack when compared to the fine-grained checking where T_c is the period of the corresponding controller task (see Table II).

¹¹We discuss this topic further in Sec. VI and Appendix G.

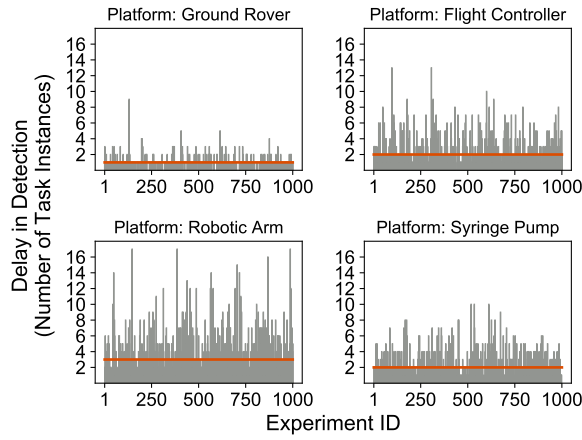


Fig. 9. Delay in detecting an intrusion (in terms of number of jobs) for SCATE in comparison with fine-grain scheme. On average (orange horizontal line), the detection delay is no more than 3 task instances for our case-study platforms.

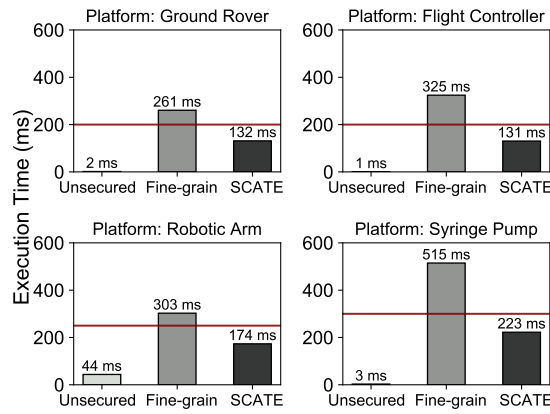


Fig. 10. Execution time of the main controller task for different schemes. The plots show 99th-percentile values observed from 1000 individual trials. Red horizontal lines represent task deadlines. Fine-grained checking requires more time to compute (due to additional checks and context switching overheads) and often derives the system in unsafe states.

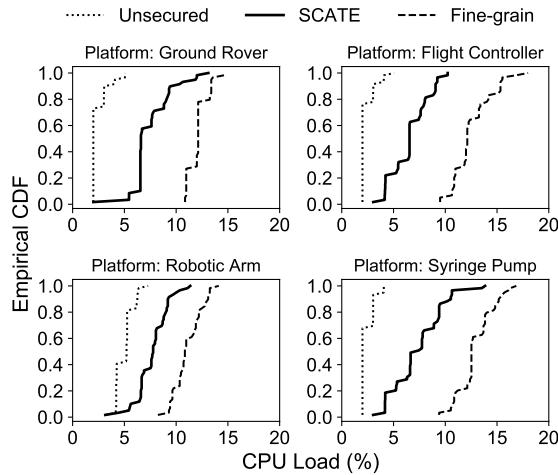


Fig. 11. Empirical CDF of the CPU load. On average, SCATE uses 30.48%–47.32% less CPU.

SCATE can provide similar-levels of security when compared to the fine-grained checking since, on-average, it requires only 1–3 additional task instances to detect the attacks.

TABLE IV
COMPARISON WITH FINE-GRAIN CHECKING: SUMMARY OF FINDINGS

Platform	Performance Metrics: SCATE vs Fine-grain			
	Execution Time Reduction (%)	CPU Usage Reduction (%)	Detection Delay (Task Instances)	
			Mean	99 th -p
Ground Rover	49.69	37.58	1	3
Flight Controller	59.81	47.32	2	8
Robotic Arm	42.80	30.48	3	12
Syringe Pump	56.81	42.87	2	8

Timeliness and Overhead Analysis: The physical system will remain stable if the controller task can finish execution before its next (periodic) invocation. As a reference, we also compare with traces from vanilla execution scenarios when there is no verification of actuation commands (*i.e.*, tasks are always running in the rich OS). We refer to this vanilla execution as “unsecured” since it does not protect the system from any adversarial actions. Figure 10 shows the execution time (y-axis) for all three schemes (captured using the Linux `clock_gettime()` function and the `CLOCK_PROCESS_CPUTIME_ID` clock). The horizontal line represents the deadlines, *i.e.*, if the response time of the task is above the margin, the task misses its deadline and the physical system will become unstable (and hence unsafe). Both the fine-grained checking and SCATE increase response times when compared to the unsecured scheme since there is no context switch between Linux and OP-TEE in the latter. We note that the increase in computing resources due to integration of additional security checking/protection techniques (*e.g.*, cryptographic operations, memory isolation, intrusion detection, control flow integrity checks) is an expected side-effect to improve security as observed in prior work [32], [34], [35], [48], [78], [79].

The fine-grained scheme expends more time (when compared to SCATE) since it verifies all N actuation commands, *i.e.*, there are more context switches (from rich OS to secure enclave) and runtime checking overheads. As a result, the controller task easily misses its deadline and drive the system into an unsafe state for all of our case-studies. In contrast, intermittent checking (SCATE) allows the tasks to finish within deadlines. We note that since, by definition, task response times must be less than their periods for stability requirements (Appendix A), the controller tasks must be required to execute with a slower frequency (*i.e.*, longer period) if we want to enforce fine-grain checking. For many control systems sampling rates affect the control performance [80]; therefore by selectively checking only a subset of commands, designers can improve task response times and control frequencies while ensuring stability of the physical system. Recall from earlier discussion (Sec. I–II) that the usefulness of real-time tasks depends on whether it finished before their deadlines (*i.e.*, earlier completion does not provide added benefits). Hence the delays due to SCATE are acceptable since deadlines are met.

Fine-grained checking increases execution times and controller tasks fail to comply with their timing requirements. SCATE manages to complete execution before the deadline of the tasks and this is by design.

In the final set of experiments (Fig. 11) we show the resource usage (*i.e.*, CPU load) for all three cases (unsecured, fine-grained and SCATE) for each platform in our evaluation. For this, we executed the controller tasks independently for 60 seconds and observed the CPU load using the `/proc/stat` interface. We report the results from 1000 individual trials. The x-axes of Fig. 11 show the CPU load and y-axes show the corresponding cumulative distribution function (CDF). From our experiments we found that SCATE increases CPU usage by 1.5–3.2 times when compared to unsecured scheme — this is expected since vanilla execution does not provide any security guarantees (and there is no additional context switch overhead). We also note that SCATE *reduces CPU load by 30.48%–47.32%* when compared to the fine-grain scheme; this could be useful for many applications (say for battery operated systems to improve thermal efficiency).

In comparison with fine-grained checking, on average, SCATE uses 30.48%–47.32% less CPU for its operations.

Our experiments on the four real platforms conclude that SCATE provides significant savings in task response time (*i.e.*, guarantees stability and ensures system safety) and resource usage but comes with a cost (*e.g.*, mean detection delay is at most 3 jobs). Table IV summarizes our findings (*i.e.*, delay in detection as well as reduction in execution time and CPU usage) for all four experimental platforms. As we see in our experiments, there is a trade-off between security and real-time requirements. For instance, the fine-grain checking scheme can detect the intrusions faster (*i.e.*, requires at most one additional instances) when compared to SCATE. However it results in the controller tasks taking significantly longer time to finish (*i.e.*, can make the system unstable) and consume more resources (*e.g.*, CPU, battery, memory). By using the mechanisms proposed in SCATE, *designers can now measure such trade-offs*, evaluate the cost of integrating security and customize the number of security checks for a task that provides the best balance between real-time and security guarantees.

TABLE V
SIMULATION PARAMETERS

Parameter	Values
Number of processor cores, P	4
Number of tasks, M	[12, 40]
Task periods, T_i	[10, 1000] ms
Number of actuation requests, N_i	{[3, 5], [8, 10]}
Minimum requests verified per job, N_i^{min}	[0.2 N_i]
Verification overhead, C_i^o	10% of C_i

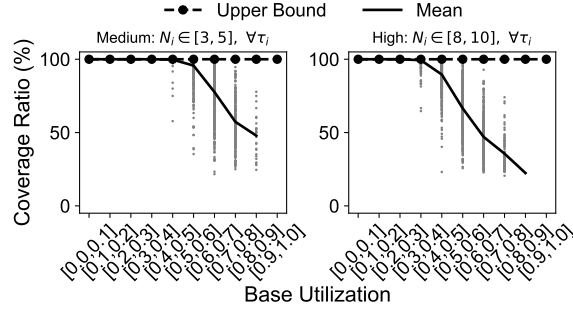


Fig. 12. Utilization vs coverage ratio. The upper bound represents fine grain checking where all the commands are verified. SCATE can provide at least 50% coverage per instance if the system utilization is no more than 70%.

C. Simulation-based Evaluation

We also developed an open source simulator [20] and conducted experiments with randomly generated workloads for a broader design-space exploration. Table V lists the parameters used in our simulations.

1) *Workload Generation*: We considered $P = 4$ cores and each taskset instance contained $[3P, 10P]$ tasks. To generate systems with an even distribution of tasks, we grouped the tasksets by base CPU utilization¹² from $[(0.01+0.1i)P, (0.1+0.1i)P]$ where $i \in \mathbb{Z}, 0 \leq i \leq 9$. Each utilization group contained 500 tasksets (*i.e.*, a total $10 \times 500 = 5000$ tasksets were tested). We assumed that the tasks were partitioned using the first-fit strategy [82]. We only considered the feasible tasksets (*i.e.*, the ones where response times are less than deadlines for all tasks) — since tasksets that fail to meet this condition are trivially unschedulable. Task periods were generated according to a log-uniform distribution where each task had periods between [10, 1000] ms. We assumed rate-monotonic priority ordering (*i.e.*, shorter period implies higher priorities) [81] since this is the standard techniques used in practical applications [83]–[86]. For a given number of tasks and total system utilization, the utilization of individual tasks were generated using Randfixedsum algorithm [87].

We further assumed that for each task τ_i , the overhead for checking each actuation command (C_i^o) is no more than 10% of task execution time C_i (*i.e.*, $C_i^o = 0.1C_i$). We considered two actuation command request scenarios: (i) medium ($N_i \in [3, 5], \forall \tau_i$) and (ii) high ($N_i \in [8, 10], \forall \tau_i$). We also assumed equal weights for all actuation commands and the minimum number of checking N_i^{min} was at least 20% of total number of requests (*i.e.*, $N_i^{min} = \lceil 0.2N_i \rceil$).

2) *Results*: In the following experiments (Fig. 12) we study how many commands can be checked in each of the task instances. For this, we introduce a metric called “coverage ratio” (CR). The CR metric shows us how many actuation commands (out of the total number of commands) we can check without violating timing constraints. We define CR as follows: $CR = \frac{1}{|\Gamma|} \sum_{\tau_i \in \Gamma} \frac{K_i}{N_i}$ where $\frac{1}{|\Gamma|} \sum_{\tau_i \in \Gamma} \frac{N_i^{min}}{N_i} \leq CR \leq 1$ $|\Gamma|$ is the total number of tasks and the parameter K_i is obtained from Algorithm 1 (see Sec. IV-B). Notice that $CR = 1$ (*i.e.*, upper bound) represents the fine-grain checking case since we verify all the commands. Let us now define base-utilization of a taskset (*i.e.*, total utilization without any actuation checking) as $\frac{U}{P}$ where $U = \sum_{\tau_i \in \Gamma} \frac{C_i}{T_i}$, C_i is the task execution time and P is the period. The x-axis of Fig. 12 shows the base-utilization and y-axis shows coverage ratio for both medium (left plot) and high (right plot) actuation scenarios. From our experiments we find that *SCATE provides a similar level of security when compared to fine-grain scheme* if the total utilization is no more than 60% and 40% for medium and high actuation request cases, respectively. We note that while fine-grain checking can provide better coverage, this upper bound is otherwise unattainable (specially for high utilization cases) since the all the tasks may not meet their timing requirements. This is seen in our additional experiments (Fig. 14). In contrast, SCATE can provide at least 50% coverage even in high utilization cases (*e.g.*, at $\frac{U}{P} \leq 0.7$), when fine-grained checking fails since it makes the system infeasible.

¹²In real-time terminology, the *utilization* of a task is given by the ratio of its execution time to period [81].

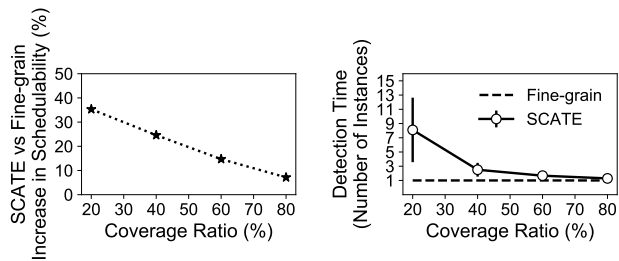


Fig. 13. Real-time and security trade-offs: low coverage ratio (*i.e.*, when fewer commands are checked in each task instance), while increasing the acceptance ratio (left plot), can lead to increase in detection time (right plot). We set the number of actuation commands at $N_i = 5$.

*The performance of SCATE is identical to the fine-grain scheme for low-to-medium system utilizations (*i.e.*, able to check all actuation commands).*

In the last set of experiments (Fig. 13) we show the trade-off between real-time and security guarantees. For this, we use the “schedulability” metric — a useful mathematical tool developed by the real-time community to analyze whether all activities of a given system can meet their timing constraints even in the worst-case behavior of the system [88]. A given taskset is considered as *schedulable* if *all* the tasks in the taskset meet their timing requirements (*i.e.*, response time is less than or equal to deadline). If the tasks are not schedulable, the system will be unsafe (and should not be deployed). The x-axis of Fig. 13 shows the coverage ratio. The y-axis in the left figure shows the increase in schedulability in SCATE when compared to the fine-grain scheme while the right figure shows the detection time (in terms of number of task instances) for both of the schemes. As we mentioned earlier, in the fine-grain scheme, the detection time for a known attack is upper bounded by the period of the task (*i.e.*, requires at most one additional instances when compared to the insecure base-case). As we see from the figure, there is a trade-off between real-time and security requirements: lower coverage ratio increases the schedulability (since there are lower checking overheads) but increases the detection times. This is because if coverage ratio is low, only a few commands are selected for checking during each instance and a vulnerable/compromised command will only be verified infrequently; thus resulting in longer detection times. We also carried out additional experiments (Appendix F) to study the trade-offs of integrating TEE-based SCATE mechanism in existing real-time platforms. Our results (see Fig. 14 in Appendix F) show that there is a cost of integrating security (since it reduces the number of tasks that meets their timing requirements).

*If we perform fewer checks in each task instance, we can accommodate more tasks in the system (*i.e.*, higher acceptance ratio). However, this may result in delayed detections (*e.g.*, on average, requires eight additional task instances) since not all the actuation commands are frequently checked.*

Summary. Our experiments reveal interesting trade-offs between real-time and security requirements. Fine-grain checking — while providing better security guarantees (*i.e.*, lower detection time) — can negatively affect schedulability and, hence, safety and integrity of the system. SCATE, in contrast, provides better schedulability guarantees (especially for high utilization cases) but may result in slower detection times. By using our approach, designers of the systems can now customize their platforms and selectively verify actuation commands based on application requirements.

VI. DISCUSSION

Our current implementation blocks malicious commands. Other strategies could involve the raising of alarms and/or sending out buffered (or even predetermined) alternate commands. SCATE transfers the control to the secure enclave for a (random) subset of actuation requests. Although this does not jeopardize the safety of the physical system (see more in the following paragraph), an adversary can still send spoofed signals in lieu of the unchecked commands (perhaps in a brute force manner). Alternative design choices (to further improve security and minimize overhead) could (*i*) pass of all the actuation requests through the trusted enclave but checks only a few commands or (*ii*) buffer multiple commands together and then transfer control *once* to the enclave for checking. We intend to incorporate these features in future work.

While SCATE adds delays in detection (*e.g.*, on average 1–3 task instances when compared to the scheme that checks all the actuation commands), we can still retain the safety and normal operations of the plant due to physical inertia. For example, consider a simplified drone example. If an adversary sends false commands and turns off the propellers, the drone’s altitude will not instantaneously drop to zero. Hence, although SCATE may not detect the attack instantly, it can still block spoofed commands and prevent the drone from crashing. We present additional results and discuss this topic further in Appendix G.

In this paper we assume the existence of “perfect” checking modules provided by the system engineers (*i.e.*, an attack is always correctly detected by the CheckAct() function). Depending on the actual implementation, CheckAct() functions may result in false-positive/false-negative errors. Our model can also handle such cases by incorporating the detection inefficiency

factors in the calculation of reward/cost metrics. For example, if the detection accuracy of `CheckAct()` is 95%, one way to express reward and cost functions is as follows: $\lambda_{\text{Imperfect}} = (1 - .05)\lambda$ and $\zeta_{\text{Imperfect}} = (1 + .05)\zeta$, respectively.

The game theory-based formulation used in our work can be extended to other real-time security use-cases. For instance, consider a distributed CPS where real-time nodes periodically exchange messages that need to be encrypted/authenticated (say to prevent man-in-the-middle attacks) [29], [78], [89]. While longer key sizes can provide better encryption, it requires more time to perform crypto operations (hence less number of messages can be secured and/or tasks can miss deadlines). By using game formulations similar to those in this paper, designers of systems can use different (perhaps smaller) key sizes for different messages (to reduce overhead) that provides maximal security from an external observer’s point of view while guaranteeing timing requirements.

Although we demonstrate our ideas on four realistic real-time platforms, the lack of real-time benchmarks is one of the major challenges in evaluating real-time cyber-physical security solutions. This is partly because of the diversity of such applications and software/hardware platforms as well as their hardware-dependent nature. In addition, critical cyber-physical applications are rarely open-sourced for safety/security/proprietary reasons. As a result, existing real-time security research is mainly evaluated by limited case-studies [6]–[8], [25], [29], [30], [33], [83]–[86], [90] and/or by using simulations [32], [78], [79], [89].

VII. RELATED WORK

Enhancing security in time-critical cyber-physical systems is an active research area [2], [91]. Perhaps the closest line of work to ours is PROTC [57] where a monitor in the enclave enforces secure access control policy (given by the control center) for some peripherals of the drone and ensures that only authorized applications can access certain peripherals. Unlike our scheme, PROTC is limited for specific applications (*i.e.*, aerial robotic vehicles), requires a centralized control center to validate/enforce security policies and does not consider any load balancing issues. In other work [83]–[86], we proposed mechanisms to secure legacy RTS by integrating additional, independent, periodic monitoring tasks. They are pure software-based solutions and do not guarantee the integrity of security checks like SCATE. In contrast, in this paper consider a TEE-based RTS where security checks (*i.e.*, actuation command verification using trusted enclave) are interleaved within real-time tasks. Researchers also proposed anomaly detection approaches for robotic vehicles [21], [35], [92]. These approaches do not leverage the capabilities of TEEs (*i.e.*, are vulnerable if the adversary can compromise the host OS) and do not consider real-time aspects. There exist various hardware/software-based mechanisms and architectural frameworks [6]–[8], [33], [90], [93], [94]. However they are not designed to protect against control-specific attacks and may not be suitable for systems developed with COTS components.

Researchers also use game-theoretical analysis for (a) general-purpose control systems [40], [42], (b) decision making problems [41] and (c) preventing physical intrusions in CPS [43]. These schemes are not designed to protect the systems against false actuation commands. In addition, they are not timing-aware (*i.e.*, real-time requirements are not considered). There also exist large number of research for generic cyber-physical/IoT-specific embedded systems as well as use of TrustZone to secure traditional embedded/mobile applications (too many to enumerate here, refer to the related surveys [14], [95]–[98]) — however the consideration of actuation-specific security scheduling and overload management aspects of real-time applications distinguish our work from other research. To the best of our knowledge, this is the first comprehensive work that introduces the notion of randomized coarse-grain checking for overloaded systems in order to validate actuation commands in a TEE-enabled real-time CPS.

VIII. CONCLUSION

In this paper we present a framework, SCATE, to enhance the security and safety of the time-critical cyber-physical systems. We use a combination of trusted hardware and the intrinsic real-time nature of such systems and propose techniques to selectively verify a subset of commands that provides a trade-offs between real-time and security guarantees. We believe that our technique can be incorporated into multiple cyber-physical application domains such as avionics, automobiles, industrial control systems, medical devices, unmanned and autonomous vehicles.

REFERENCES

- [1] K. Castelli, A. M. A. Zaki, and H. Giberti, “Development of a practical tool for designing multi-robot systems in pick-and-place applications,” *MDPI Robotics*, vol. 8, no. 3, 2019.
- [2] C.-Y. Chen, M. Hasan, and S. Mohan, “Securing real-time Internet-of-things,” *Sensors*, vol. 18, no. 12, 2018.
- [3] A. O. Otuoze, M. W. Mustafa, and R. M. Larik, “Smart grids security challenges: Classification by sources of threats,” *Elsevier JESIT*, vol. 5, no. 3, pp. 468–483, 2018.
- [4] P. Zheng, Z. Sang, R. Y. Zhong, Y. Liu, C. Liu, K. Mubarak, S. Yu, X. Xu *et al.*, “Smart manufacturing systems for Industry 4.0: Conceptual framework, scenarios, and future perspectives,” *Springer Front. of Mech. Eng.*, vol. 13, no. 2, pp. 137–150, 2018.
- [5] H. F. Azgomi and M. Jamshidi, “A brief survey on smart community and smart transportation,” in *IEEE ICTAI*, 2018, pp. 932–939.
- [6] M.-K. Yoon, S. Mohan, J. Choi, J.-E. Kim, and L. Sha, “SecureCore: A multicore-based intrusion detection architecture for real-time embedded systems,” in *IEEE RTAS*, 2013, pp. 21–32.
- [7] F. Abdi, C.-Y. Chen, M. Hasan, S. Liu, S. Mohan, and M. Caccamo, “Preserving physical safety under cyber attacks,” *IEEE IoT J.*, vol. 6, no. 4, pp. 6285–6300, 2018.
- [8] S. Mohan, S. Bak, E. Betti, H. Yun, L. Sha, and M. Caccamo, “S3A: Secure system simplex architecture for enhanced security and robustness of cyber-physical systems,” in *ACM HiCoNS*. ACM, 2013, pp. 65–74.

- [9] N. Falliere, L. O. Murchu, and E. Chien, “W32. stuxnet dossier,” *White paper, Symantec Corp.*, vol. 5, p. 6, 2011.
- [10] S. S. Clark and K. Fu, “Recent results in computer security for medical devices,” in *MobiHealth*, 2011, pp. 111–118.
- [11] S. Checkoway, D. McCoy, B. Kantor, D. Anderson, H. Shacham, S. Savage, K. Koscher, A. Czeskis, F. Roesner, T. Kohno *et al.*, “Comprehensive experimental analyses of automotive attack surfaces,” in *USENIX Sec. Symp.*, 2011.
- [12] J. Westling, “Future of the Internet of things in mission critical applications,” 2016.
- [13] E. Simmon, K.-S. Kim, E. Subrahmanian, R. Lee, F. De Vaulx, Y. Murakami, K. Zetsu, and R. D. Sriram, *A vision of cyber-physical cloud computing for smart networked systems*. US Dept. of Commerce, NIST, 2013.
- [14] S. Pinto and N. Santos, “Demystifying ARM TrustZone: A comprehensive survey,” *ACM CSUR*, vol. 51, no. 6, p. 130, 2019.
- [15] V. Costan and S. Devadas, “Intel SGX Explained,” *IACR Crypt. ePrint Arch.*, no. 086, pp. 1–118, 2016.
- [16] J. C. Harsanyi and R. Selten, “A generalized nash solution for two-person bargaining games with incomplete information,” *INFORMS Man. Sci.*, vol. 18, no. 5-part-2, pp. 80–106, 1972.
- [17] V. Conitzer and T. Sandholm, “Computing the optimal strategy to commit to,” in *ACM EC*, 2006, pp. 82–90.
- [18] P. Paruchuri, J. P. Pearce, M. Tambe, F. Ordonez, and S. Kraus, “An efficient heuristic approach for security against multiple adversaries,” in *IFAAMAS AAMAS*, 2007, pp. 1–8.
- [19] “Raspberry Pi,” <https://tinyurl.com/rpi3modelb>.
- [20] “SCATE implementation,” https://github.com/mnwrhsn/scate_implementation.
- [21] P. Guo, H. Kim, N. Virani, J. Xu, M. Zhu, and P. Liu, “RoboADS: Anomaly detection against sensor and actuator misbehaviors in mobile robots,” in *IEEE/IFIP DSN*, 2018, pp. 574–585.
- [22] “Dexter Industries Sensors,” https://github.com/DexterInd/DI_Sensors.
- [23] “I²C manual,” Philips Semiconductors, 2003. [Online]. Available: <https://tinyurl.com/i2c-manual>
- [24] R. Mahfouzi, A. Aminifar, S. Samii, M. Payer, P. Eles, and Z. Peng, “Butterfly attack: Adversarial manipulation of temporal properties of cyber-physical systems,” in *IEEE RTSS*, 2019, pp. 93–106.
- [25] M. Hasan and S. Mohan, “Protecting actuators in safety critical IoT systems from control spoofing attacks,” in *ACM IoT S&P*, 2019, pp. 8–14.
- [26] C.-Y. Chen, S. Mohan, R. Pellizzoni, R. B. Bobba, and N. Kiyavash, “A novel side-channel in real-time schedulers,” in *IEEE RTAS*, 2019, pp. 90–102.
- [27] S. Liu, N. Guan, D. Ji, W. Liu, X. Liu, and W. Yi, “Leaking your engine speed by spectrum analysis of real-time scheduling sequences,” *J. of Sys. Arch.*, vol. 97, pp. 455–466, 2019.
- [28] M. Bechtel and H. Yun, “Denial-of-service attacks on shared cache in multicore: Analysis and prevention,” in *IEEE RTAS*, 2019, pp. 357–367.
- [29] V. Lesi, I. Jovanov, and M. Pajic, “Network scheduling for secure cyber-physical systems,” in *IEEE RTSS*, 2017, pp. 45–55.
- [30] V. Lesi, I. Jovanov, and M. Pajic, “Security-aware scheduling of embedded control tasks,” *ACM TECS*, vol. 16, pp. 188:1–188:21, 2017.
- [31] F. Loi, A. Sivanathan, H. H. Gharakheili, A. Radford, and V. Sivaraman, “Systematically evaluating security and privacy for consumer IoT devices,” in *ACM IoTS&P*, 2017, pp. 1–6.
- [32] R. Pellizzoni, N. Paryab, M.-K. Yoon, S. Bak, S. Mohan, and R. B. Bobba, “A generalized model for preventing information leakage in hard real-time systems,” in *IEEE RTAS*, 2015, pp. 271–282.
- [33] M.-K. Yoon, S. Mohan, J. Choi, M. Christodorescu, and L. Sha, “Learning execution contexts from system call distribution for anomaly detection in smart embedded system,” in *ACM/IEEE IoTDI*, 2017, pp. 191–196.
- [34] C. H. Kim, T. Kim, H. Choi, Z. Gu, B. Lee, X. Zhang, and D. Xu, “Securing real-time microcontroller systems through customized memory view switching,” in *NDSS*, 2018.
- [35] H. Choi, W.-C. Lee, Y. Aafer, F. Fei, Z. Tu, X. Zhang, D. Xu, and X. Xinyan, “Detecting attacks against robotic vehicles: A control invariant approach,” in *ACM CCS*, 2018, pp. 801–816.
- [36] A. Hussain, M. Hannan, A. Mohamed, H. Sanusi, and A. Ariffin, “Vehicle crash analysis for airbag deployment decision,” *Int. J. of Auto. Tech.*, vol. 7, no. 2, pp. 179–185, 2006.
- [37] T. Roughgarden, “Algorithmic game theory,” *Comm. of the ACM*, vol. 53, no. 7, pp. 78–86, 2010.
- [38] Y. A. Korilis, A. A. Lazar, and A. Orda, “Achieving network optima using Stackelberg routing strategies,” *IEEE/ACM TON*, vol. 5, no. 1, pp. 161–173, 1997.
- [39] J. Cardinal, M. Labbé, S. Langerman, and B. Palop, “Pricing of geometric transportation networks,” in *CCCG*, 2005, pp. 92–96.
- [40] S. Moothedath, D. Sahabandu, J. Allen, A. Clark, L. Bushnell, W. Lee, and R. Poovendran, “A game-theoretic approach for dynamic information flow tracking to detect multi-stage advanced persistent threats,” *IEEE TACON*, 2020.
- [41] G. Yang, R. Poovendran, and J. P. Hespanha, “Adaptive learning in two-player stackelberg games with continuous action sets,” in *IEEE CDC*, 2019, pp. 6905–6911.
- [42] J. Chen and Q. Zhu, “A game-theoretic framework for resilient and distributed generation control of renewable energies in microgrids,” *IEEE Trans. on Smart Grid*, vol. 8, no. 1, pp. 285–295, 2016.
- [43] S. Rass, A. Alshawish, M. A. Abid, S. Schauer, Q. Zhu, and H. De Meer, “Physical intrusion games—optimizing surveillance by simulation and game theory,” *IEEE Access*, vol. 5, pp. 8394–8407, 2017.
- [44] T. Yu, V. Sekar, S. Seshan, Y. Agarwal, and C. Xu, “Handling a trillion (unfixable) flaws on a billion devices: Rethinking network security for the Internet-of-things,” in *ACM HotNets*, 2015, pp. 1–7.
- [45] S. Adepou and A. Mathur, “From design to invariants: Detecting attacks on cyber physical systems,” in *IEEE QRS-C*, 2017, pp. 533–540.
- [46] R. Berthier and W. H. Sanders, “Specification-based intrusion detection for advanced metering infrastructures,” in *IEEE PRDC*. IEEE, 2011, pp. 184–193.
- [47] V. Chandola, A. Banerjee, and V. Kumar, “Anomaly detection: A survey,” *ACM CSUR*, vol. 41, no. 3, p. 15, 2009.
- [48] A. Mukherjee, T. Mishra, T. Chantem, N. Fisher, and R. Gerdes, “Optimized trusted execution for hard real-time applications on cots processors,” in *ACM RTNS*, 2019, pp. 50–60.
- [49] J. Amacher and V. Schiavoni, “On the performance of arm trustzone,” in *IFIP DAIS*, 2019, pp. 133–151.
- [50] Y. Liu, K. An, and E. Tilevich, “RT-trust: Automated refactoring for trusted execution under real-time constraints,” in *ACM GPCE*, 2018, pp. 175–187.
- [51] “Open Portable Trusted Execution Environment,” <https://www.op-tee.org/>.
- [52] “ARM Fixed Virtual Platforms,” <https://developer.arm.com/tools-and-software/simulation-models/fixe-virtual-platforms>.
- [53] “FreeRTOS,” <http://www.freertos.org>.
- [54] N. Audsley, A. Burns, M. Richardson, K. Tindell, and A. J. Wellings, “Applying new scheduling theory to static priority pre-emptive scheduling,” *SE Journal*, vol. 8, no. 5, pp. 284–292, 1993.
- [55] L. Cheng, K. Tian, and D. D. Yao, “Orpheus: Enforcing cyber-physical execution semantics to defend against data-oriented attacks,” in *ACM ACSAC*, 2017, pp. 315–326.
- [56] R. Liu and M. Srivastava, “VirtSense: Virtualize Sensing through ARM TrustZone on Internet-of-Things,” in *ACM SysTEX*, 2018, pp. 2–7.
- [57] R. Liu and M. Srivastava, “PROTC: PROTeCting drone’s peripherals through ARM trustzone,” in *ACM DroNet*, 2017, pp. 1–6.
- [58] T. Liu, A. Hojjati, A. Bates, and K. Nahrstedt, “Alidrone: Enabling trustworthy proof-of-alibi for commercial drone compliance,” in *IEEE ICDCS*, 2018, pp. 841–852.

- [59] “Adafruit motor shield,” <https://learn.adafruit.com/adafruit-motor-shield>.
- [60] “Adafruit driver,” https://github.com/threebrooks/AdafruitStepperMotorHAT_CPP.
- [61] “PCA9685 I2C PWM driver,” <https://github.com/TeraHz/PCA9685>.
- [62] “TEE API,” <https://globalplatform.org/specs-library/tee-client-api-specification/>.
- [63] “The Python-MIP package,” <https://www.python-mip.com/>.
- [64] K. Martin, “Tutorial: COIN-OR: Software for the OR community,” *INFORMS Interfaces*, vol. 40, no. 6, pp. 465–476, 2010.
- [65] A. Lipowski and D. Lipowska, “Roulette-wheel selection via stochastic acceptance,” *Elsevier Physica A*, vol. 391, no. 6, pp. 2193–2196, 2012.
- [66] “Z1FFER open source hardware random number generator,” <http://www.openrandom.org>.
- [67] “Open hardware random number generator,” <https://onerng.info>.
- [68] M. R. Aliabadi, A. A. Kamath, J. Gascon-Samson, and K. Pattabiraman, “Artinali: dynamic invariant detection for cyber-physical system security,” in *ACM ESEC/FSE*, 2017, pp. 349–361.
- [69] F. M. Tabrizi and K. Pattabiraman, “Flexible intrusion detection systems for memory-constrained embedded systems,” in *IEEE EDCC*, 2015, pp. 1–12.
- [70] F. Abdi, C.-Y. Chen, M. Hasan, S. Liu, S. Mohan, and M. Caccamo, “Guaranteed physical security with restart-based design for cyber-physical systems,” in *ACM/IEEE ICCPS*, 2018, pp. 10–21.
- [71] “Raspberry Pi rover,” <https://github.com/Veilkrand/simplePiRover>.
- [72] “GoPiGo,” <https://github.com/DexterInd/GoPiGo>.
- [73] “Drone controller,” <https://github.com/lobodol/drone-flight-controller>.
- [74] K. J. Åström and T. Hägglund, “Revisiting the Ziegler–Nichols step response method for PID control,” *Elsevier J. of proc. con.*, vol. 14, no. 6, pp. 635–650, 2004.
- [75] “Robot arm control,” <https://github.com/tutRPi/6DOF-Robot-Arm>.
- [76] “C-FLAT implementation,” <https://github.com/control-flow-attestation/c-flat>.
- [77] T. Abera, N. Asokan, L. Davi, J.-E. Ekberg, T. Nyman, A. Paverd, A.-R. Sadeghi, and G. Tsudik, “C-FLAT: control-flow attestation for embedded systems software,” in *ACM CCS*, 2016, pp. 743–754.
- [78] T. Xie and X. Qin, “Improving security for periodic tasks in embedded systems through scheduling,” *ACM TECS*, vol. 6, no. 3, p. 20, 2007.
- [79] S. Mohan, M.-K. Yoon, R. Pellizzoni, and R. B. Bobba, “Real-time systems security through scheduler constraints,” in *Euromicro ECRTS*, 2014, pp. 129–140.
- [80] E. Bini and A. Cervin, “Delay-aware period assignment in control systems,” in *IEEE RTSS*, 2008, pp. 291–300.
- [81] C. L. Liu and J. W. Layland, “Scheduling algorithms for multiprogramming in a hard-real-time environment,” *JACM*, vol. 20, no. 1, pp. 46–61, 1973.
- [82] J. Chen, “Partitioned multiprocessor fixed-priority scheduling of sporadic real-time tasks,” in *Euromicro ECRTS*, 2016, pp. 251–261.
- [83] M. Hasan, S. Mohan, R. B. Bobba, and R. Pellizzoni, “Exploring opportunistic execution for integrating security into legacy hard real-time systems,” in *IEEE RTSS*, 2016, pp. 123–134.
- [84] M. Hasan, S. Mohan, R. Pellizzoni, and R. B. Bobba, “Contego: An adaptive framework for integrating security tasks in real-time systems,” in *Euromicro ECRTS*, 2017, pp. 23:1–23:22.
- [85] M. Hasan, S. Mohan, R. Pellizzoni, and R. B. Bobba, “A design-space exploration for allocating security tasks in multicore real-time systems,” in *DATE*, 2018, pp. 225–230.
- [86] M. Hasan, S. Mohan, R. Pellizzoni, and R. B. Bobba, “Period adaptation for continuous security monitoring in multicore systems,” in *DATE*, 2020.
- [87] P. Emberson, R. Stafford, and R. I. Davis, “Techniques for the synthesis of multiprocessor tasksets,” in *WATERS*, 2010, pp. 6–11.
- [88] R. I. Davis and A. Burns, “A survey of hard real-time scheduling for multiprocessor systems,” *ACM CSUR*, vol. 43, no. 4, pp. 35:1–35:44, 2011.
- [89] M. Lin, L. Xu, L. T. Yang, X. Qin, N. Zheng, Z. Wu, and M. Qiu, “Static security optimization for real-time systems,” *IEEE Trans. on Indust. Info.*, vol. 5, no. 1, pp. 22–37, 2009.
- [90] M.-K. Yoon, S. Mohan, J. Choi, and L. Sha, “Memory heat map: anomaly detection in real-time embedded systems using memory behavior,” in *ACM/EDAC/IEEE DAC*, 2015, pp. 1–6.
- [91] H. Chai, G. Zhang, J. Zhou, J. Sun, L. Huang, and T. Wang, “A short review of security-aware techniques in real-time embedded systems,” *J. of Cir. Sys. and Comp.*, vol. 28, no. 02, 2019.
- [92] F. Fei, Z. Tu, R. Yu, T. Kim, X. Zhang, D. Xu, and X. Deng, “Cross-layer retrofitting of UAVs against cyber-physical attacks,” in *IEEE ICRA*, 2018, pp. 550–557.
- [93] F. Abdi, M. Hasan, S. Mohan, D. Agarwal, and M. Caccamo, “ReSecure: A restart-based security protocol for tightly actuated hard real-time systems,” in *IEEE CERTS*, 2016, pp. 47–54.
- [94] D. Lo, M. Ismail, T. Chen, and G. E. Suh, “Slack-aware opportunistic monitoring for real-time systems,” in *IEEE RTAS*, 2014, pp. 203–214.
- [95] A. Humayed, J. Lin, F. Li, and B. Luo, “Cyber-physical systems security – A survey,” *IEEE IoT J.*, vol. 4, no. 6, pp. 1802–1831, 2017.
- [96] Y. Yang, L. Wu, G. Yin, L. Li, and H. Zhao, “A survey on security and privacy issues in Internet-of-Things,” *IEEE IoT J.*, vol. 4, no. 5, pp. 1250–1258, 2017.
- [97] M. Ammar, G. Russello, and B. Crispo, “Internet of Things: A survey on the security of IoT frameworks,” *Elsevier J. of Inf. Sec. & App.*, vol. 38, pp. 8–27, 2018.
- [98] W. Li, H. Chen, and H. Chen, “Research on ARM TrustZone,” *ACM GetMobile*, vol. 22, no. 3, pp. 17–22, 2019.
- [99] F. Kolnick, “The QNX 4 real-time operating system,” *Basis Comp. Sys. Inc.*, 1998.
- [100] G. Heiser and B. Leslie, “The OKL4 microvisor: Convergence point of microkernels and hypervisors,” in *ACM APSys*. ACM, 2010, pp. 19–24.
- [101] L. Fu and R. Schwebel, “Real-time Linux wiki,” https://rt.wiki.kernel.org/index.php/rt_preempt_howto, [Online].
- [102] R. Wilhelm, J. Engblom, A. Ermedahl, N. Holsti, S. Thesing, D. Whalley, G. Bernat, C. Ferdinand, R. Heckmann, T. Mitra *et al.*, “The worst-case execution-time problem—overview of methods and survey of tools,” *ACM TECS*, vol. 7, no. 3, p. 36, 2008.
- [103] D. Isov, “Handling sporadic tasks in real-time systems: Combined offline and online approach,” Tech. Rep., June 2001.
- [104] L. Vandenberghe, “The CVXOPT linear and quadratic cone program solvers,” 2010. [Online]. Available: <http://cvxopt.org/documentation/coneprog.pdf>
- [105] T. Luukkonen, “Modelling and control of quadcopter,” School of Science, Aalto University, Tech. Rep., 2011.

APPENDIX

A. System Model: Real-Time Task Model and Scheduling

We consider a system that consists of M fixed-priority real-time tasks $\Gamma = \{\tau_i, \dots, \tau_M\}$ running on P identical processor cores $\Pi = \{\pi_1, \dots, \pi_P\}$. In this work, we consider partitioned fixed-priority preemptive scheduling [88] (a widely supported approach in many commercial and open-source real-time operating systems such as QNX [99], OKL4 [100], real-time Linux [101], *etc.*) where tasks are statically assigned to the processor cores using a predefined partitioning scheme. The

TABLE VI
REAL-TIME TERMINOLOGY

Term	Interpretation
Deadline	Real-time constraint of a task. Tasks must finish their computation before deadlines to ensure the safe operation of the system
Period	Inter-arrival time of a task. Each task instance (also called “job”) periodically performs desired computation
Schedulability	Mathematical tool to determine whether all tasks can meet their timing constraints (deadlines) even in the worst-case behavior of the system
Utilization	Ratio between task execution time to its period
Worst-case execution time (WCET)	An upper bound of the task execution time, determined at the system design phase
Worst-case response time (WCRT)	Time between task arrival to completion. WCRT must be less than the deadline of the tasks to ensure schedulability

TABLE VII
ACTUATION COMMAND CHECKING FOR VARIOUS CYBER-PHYSICAL PLATFORMS*

Platform	Application	Actuators	Possible Checking Conditions
Robotic vehicle (ground, aerial)	Surveillance, agriculture, manufacturing	Servo, motor	(a) Check if the robot is following the mission; (b) allow only predefined number of actuation commands per period
Robotic arm	Manufacturing	Servo, buzzer	(a) Check the servo pulse sequences matches with the desired (design-time) sequence; (b) do not raise alarm if the pulse sequence is normal
Infusion/Syringe pump	Health-care	Motor, display	(a) Drive the motor only to allowable positions/rates (b) display only the amount of fluid infused (e.g., obtained from motor encoders)
Water/air monitoring system	Home/industrial automation	Buzzer, display	(a) Send high pulse to buzzer only if water-level is high/air quality abnormal/detect smoke; (b) do not display alert if the system state is normal
Surveillance system	Home/industrial automation	Servo, buzzer	(a) Trigger alarm only if there is an impact/object detected in camera; (b) rotate camera (using servos) only within allowable pan/tilt angle

*Platforms listed in shaded rows are implemented and evaluated in this work. Other examples are presented here to illustrate applicability of our ideas for multiple use-cases.

set of tasks running on a given core π_p is denoted by Γ_p and $\Gamma = \cup_{\pi_p \in \Pi} \{\Gamma_p\}$. Each task τ_i is represented by the following tuple:

$$(C_i, T_i, D_i, N_i, N_i^{min}, W_i).$$

Each of the above variables represents the following:

- C_i is the constant, upper bound on the computation time, called worst-case execution time (WCET) [102];
- T_i is the minimum inter-arrival time (period), *i.e.*, consecutive jobs of τ_i should be temporally separated by at least T_i time units;
- D_i (usually less than or equal to T_i) is the timing constraint (deadline);
- N_i is the number of actuation requests that τ_i sends out;
- $N_i^{min} \leq N_i$ is a QoS parameter that denotes the minimum number of actuation commands that must be checked; and
- $W_i = \{\omega_i^1, \dots, \omega_i^{N_i}\}$ is a designer-provided weight vector where the weight ω_i^j represents the importance of j -th actuation command.

As shown in Sec. IV, parameters N_i^{min} and W_i help the designers to determine the subset of commands to be selected in each iteration of the task for checking when not all N_i commands can be checked due to timing constraints. While we present the above task model for ease of presentation, we note that not all the real-time tasks in a given system will send out actuation requests. For such tasks $\tau_{i'}$ setting $N_{i'} = N_{i'}^{min} = 0$ and ignoring the variable $W_{i'}$ will retain the consistency of the model.

We consider a discrete time model [103] where the system and task parameters are multiples of a fixed time unit, *i.e.*, an interval starting from time point t_1 and ending at time point t_2 that has a length of $t_2 - t_1$ by $[t_1, t_2)$ or $[t_1, t_2 - 1]$. We also assume that the non-secure system (*i.e.*, when there is no checking) is “schedulable”, that is, for each task $\tau_i \in \Gamma$, the response time (time between completion and arrival) is less than the deadline of the task. Table VI summarizes the real-time terminology used in the paper.

B. Examples of Checking Actuation Commands for Various Platforms

Table VII shows examples of conditions for actuation commands for various cyber-physical platforms.

C. Feasibility Conditions

Let N_i be the number of actuation requests generated by task τ_i that require vetting and C_i^o be an upper bound of additional computing time required due to (a) context switching (from normal execution to secure enclave and returning the context back to normal mode) and (b) performing the checks inside the enclave. Then the execution time of τ_i can be represented as

$C_i^{TEE} = C_i + N_i C_i^o$. The task τ_i is “schedulable” if the worst-case response time (WCRT), R_i^{TEE} , is less than deadline, *i.e.*, $R_i^{TEE} \leq D_i$. We can calculate an upper bound of R_i^{TEE} using traditional response-time analysis [82] as follows:

$$R_i^{TEE} = \overbrace{C_i^{TEE}}^{\text{task execution time}} + \underbrace{\sum_{\tau_h \in hp(\tau_i, \pi_p)} \left(1 + \frac{D_i}{T_h}\right) C_h^{TEE}}_{\text{interference from high-priority tasks}} \quad (3)$$

where $hp(\tau_i, \pi_p) \in \Gamma_p$ denotes the set of tasks that are higher-priority than τ_i running on core π_p . The taskset Γ is referred to as schedulable if all the tasks are schedulable, *viz.*, $R_i^{TEE} \leq D_i, \forall \tau_i \in \Gamma$.

Let $R_i = C_i + \sum_{\tau_h \in hp(\tau_i, \pi_p)} \left(1 + \frac{D_i}{T_h}\right) C_h$ denotes the vanilla response time (*i.e.*, when there is no checking). Notice that the task τ_i will miss its deadline if $R_i^{TEE} > D_i$. From Eq. (3) we can deduce that τ_i will miss its deadline if the following condition holds: $O_i > D_i - R_i$ where $O_i = N_i C_i^o + \sum_{\tau_h \in hp(\tau_i, \pi_p)} \left(1 + \frac{D_i}{T_h}\right) N_i C_h^o$ is the total overhead for checking the actuation commands including context switching in/out of the secure enclave.

D. Linear Programming Formulation for solving the Game

We can obtain the probability distributions for selecting the elements from X_i (*i.e.*, the set of all combinations of choosing K_i requests from total N_i actuation commands) for a given attacker strategy l (that maximizes the system reward) by forming the following linear program:

$$\max_{x_i^j} \sum_{j=1}^{|X_i|} x_i^j \lambda_i^{j,l} \quad (4a)$$

$$\text{s.t.} \quad \forall l' \in [1, |Q_i|], \quad \sum_{j=1}^{|X_i|} x_i^j \zeta_i^{j,l} \geq \sum_{j=1}^{|X_i|} x_i^j \zeta_i^{j,l'} \quad (4b)$$

$$\sum_{j=1}^{|X_i|} x_i^j = 1 \quad (4c)$$

$$x_i^j > 0, \quad \forall j \in [1, |X_i|] \quad (4d)$$

The objective function in Eq. (4a) maximizes the total system reward. The constraint in Eq. (4b) ensures that the current (*e.g.*, l -th) strategy results in higher cost for the attacker when compared to other adversarial strategies. The constraint in Eq. (4c) ensures the sum of probability distributions equal to unity and the last constraint in Eq. (4d) ensures non-zero probabilities so that all combinations of the actuation commands from X_i can be selected.

Let $[x_i^j]_{j=1:|X_i|}(l)$ denote the solution obtained from the linear programming formulation for the l -th adversarial strategy. Then, from all feasible strategies l (where $1 \leq l \leq |Q_i|$) we choose the one (say l^*) that maximizes the objective value in Eq. (4a), *i.e.*, $l^* = \operatorname{argmax}_{1 \leq l \leq |Q_i|} \sum_{j=1}^{|X_i|} x_i^j \lambda_i^{j,l}$. The variables $[x_i^j]_{j=1:|X_i|}(l^*)$ obtained by solving the corresponding linear program gives us the probability distributions of selecting K_i subset of commands from a total of N_i commands. The game-theoretical analysis shows that the probability distributions obtained by solving the l^* -th linear program will be optimal for the task τ_i (*i.e.*, maximizes system reward) [17], [18].

For a given strategy l , the above linear programming formulation can be solved using standard off-the-shelf optimization solvers [63], [104] in polynomial time. Since the strategy set Q_i is finite by definition, we can calculate the optimal probability distributions (*e.g.*, $[x_i^j]_{j=1:|X_i|}(l^*)$) in a finite amount of time since it is polynomial in the total number of adversarial strategies.

E. Calculation of Maximum Feasible Number of Commands

The pseudocode for calculating the maximum number of commands (K_i) that can be checked per job while guaranteeing feasibility is presented in Algorithm 2.

F. Design-time Tests for Integrating Actuation Checking in Existing Systems

We also performed experiments to show the impact of integrating TEE-based actuation checking mechanisms (*e.g.*, SCATE and the fine-grain scheme) in an existing system. For this, we use the “schedulability” metric introduced in Sec. V-C2. To demonstrate the effect of schedulability for a large number of tasksets with different parameters, let us now introduce the notion of *acceptance ratio* that is defined as the number of schedulable tasksets over the total number of generated tasksets (*e.g.*, 500 for a given utilization group in our setup as explained in Sec. V-C).

In Fig. 14 we compare the performance of difference schemes in terms of acceptance ratio (y-axis in the figure). The x-axis shows the normalized base-utilization $\frac{U}{P}$ where $U = \sum_{\tau_i \in \Gamma} \frac{C_i}{T_i}$ (*i.e.*, taskset utilization without any actuation checking). As expected, schedulability drops for high utilization cases since less number of tasks meet their deadlines due to increased

Algorithm 2 Calculation of Maximum Feasible Actuation Requests for a Given Task $\tau_i \in \Gamma_p$

```

1: Define  $K_i^l := N_i^{min}$ ,  $K_i^r := N_i$ ,  $K_i^c := 0$ 
2: Set  $\hat{\mathcal{K}}_i := \{N_i^{min}\}$  /* Initialize a variable to store feasible values */
3: while  $K_i^l \leq K_i^r$  do
4:   Update  $K_i^c := \lfloor \frac{K_i^l + K_i^r}{2} \rfloor$ 
5:   if  $\exists \tau_l \in lp(\tau_i, \pi_p)$  such that  $\tau_l$  is not schedulable with  $K_i = K_i^c$  then
6:     /* Decrease verification load to make the taskset schedulable */
7:     Update  $K_i^r := K_i^c - 1$ 
8:   else
9:     /* Taskset is schedulable with  $K_i^c$  */
10:     $\hat{\mathcal{K}}_i := \hat{\mathcal{K}}_i \cup \{K_i^c\}$  /* Add  $K_i^c$  to the feasible list */
11:    /* Check schedulability with larger  $K_i$  for next iteration */
12:    Update  $K_i^l := K_i^c + 1$ 
13:  end if
14: end while
15: /* return the maximum from the set of feasible values */
16: return  $\max(\hat{\mathcal{K}}_i)$ 

```

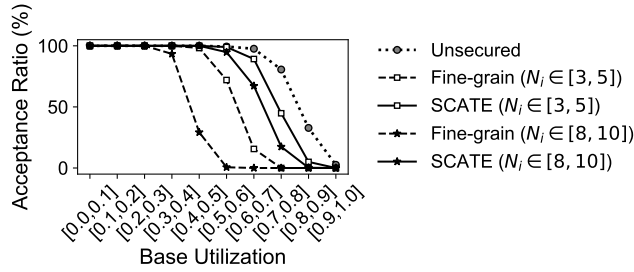


Fig. 14. Impact on schedulability for the three schemes: (i) Unsecured (does not check any actuation commands), (ii) Fine-grain (checks all the commands) and (iii) SCATE (selectively checks a subset of commands). We varied the number of actuation commands (N_i) and considered the following two scenarios: $N_i \in [3, 5]$ and $N_i \in [8, 10]$, $\forall \tau_i \in \Gamma$. Fine-grained checking can reduce schedulability significantly (specially if tasks have large number of actuation requests) due to increased validation overheads.

load. While non-secure execution (*i.e.*, when there is no command verification) results in better schedulability due to reduced utilization, it *does not provide any security guarantee*. The fine-grain checking, while providing better security (since it verifies every request), performs poorly in terms of meeting the timing guarantees specifically for highly loaded systems. (*i.e.*, less number of tasks found to be schedulable) due to more validation overheads. In contrast, SCATE provides better schedulability with (slight) QoS/security degradation as we demonstrate in Sec. V-C2. The designers of the systems can use the results presented here to analyze the feasibility of integrating TEE-based checking method in their target platforms.

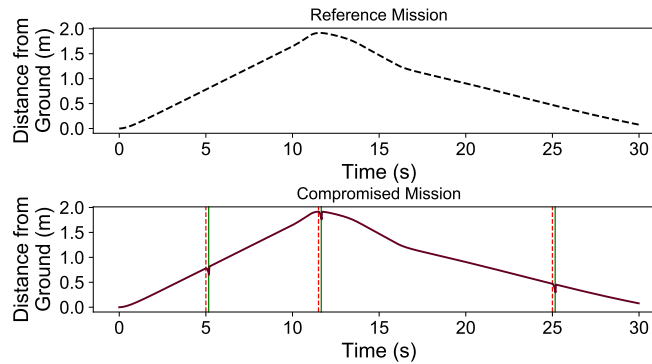


Fig. 15. Effect of physical inertia in cyber-physical applications. The top plot shows the expected altitudes of the drone during mission. The bottom plot presents the altitudes during attacks. Red dashed vertical lines show the time instance when the attack is triggered and green solid vertical lines show the time instance when SCATE detects it. While there exist slight drifts in altitudes due to delayed detection (between red and green vertical lines in the right plot), it does not jeopardize the safety (*i.e.*, the drone did not crash).

G. Impact of Physical Inertia

We now present the impact of physical inertia for detecting attacks in SCATE. For instance, consider a simple drone example. The baseline safety requirement for a drone is to not crash into the ground. We use existing quad-copter models [105] and simulate the dynamics of the drone for 30 seconds (x-axis in Fig. 15). In this mission, the drone takes-off from the ground and then lands in the target position. The y-axis in Fig. 15 represent altitudes of the drone (*i.e.*, distance from the ground) during the mission. The top plot of Fig. 15 shows the corresponding altitudes over time during the normal quad-copter operation. To demonstrate malicious activity, we injected attacks that sent false commands to turn off the propellers (bottom plot of Fig. 15). In particular, we triggered attacks at the following three points in time (red, vertical lines in the bottom side plot), (*i*) while the quad-copter was ascending (at 5 sec.), (*ii*) at the peak altitude (at 12 sec.) and (*iii*) during descent (at 25 sec.). The attacks were detected by SCATE within 8 task instances each (*i.e.*, 99-th percentile values obtained from the flight controller case-study, see Table IV). The vertical lines in the plot represent time difference when an attack is triggered (dashed red) and when it is detected (solid green) by SCATE. As the figure illustrates, there is a slight drift in altitude before SCATE detects and blocks false commands. However, this delayed detection does not jeopardize safety constraints (*i.e.*, it does not drop the drone's altitude to zero) and the drone is able to complete the mission without crashing. Hence it is not inconceivable that the detection delays induced by SCATE will be acceptable for many cyber-physical applications.